



1 **A first estimation of the contraction related to vertical axis**
2 **rotation: the case of the Ibero-Armorican Arc formation**

3 Josep Maria Casas^{1*}, Joan Guimerà¹⁻², Joaquina Alvarez-Marron³, Ícaro Días da Silva⁴⁻⁵

4 ¹ *Dpt. de Dinàmica de la Terra i de l'Oceà, Universitat de Barcelona, Martí Franquès s/n, 08028 Barcelona, Spain,*
5 *casas@ub.edu, joan.guimera@ub.edu*

6 ² *Institut de recerca GEOMODELS, Martí Franquès s/n, 08028 Barcelona, Spain.*

7 ³ *Dpt. of Earth Structure and Dynamics, and Crystallography, Institute of Earth Sciences, Jaume Almera, CSIC,*
8 *Lluís Solé i Sabarís s/n, 08028 Barcelona, Spain, jalvarez@ictja.csic.es*

9 ⁴ *Instituto Dom Luiz (IDL), Faculdade de Ciências, Universidade de Lisboa, Campo Grande, Edif. C1, Piso 1, 1749-*
10 *016 Lisboa, Portugal, ipicaparopo@gmail.com*

11 ⁵ *Dpto. de Geologia, Faculdade de Ciências, Universidade de Lisboa, Campo Grande, 1749-016 Lisboa, Portugal,*
12 *ipicaparopo@gmail.com*

13

14 * *Corresponding author (e-mail: casas@ub.edu)*

15 **Abstract.** Different models have been proposed to explain the formation of the Ibero-Armorican Arc, which require
16 significant vertical axis rotations, at the end of the Variscan orogeny. Estimates of the amount of contraction
17 (horizontal shortening) needed for these rotations range from 54% to 91% perpendicularly to the arc. These
18 estimates are compared with coeval deformational structures developed in two areas of the orogen, one in the
19 autochthonous hinterland underlying the Galicia-Trás-os-Montes Zone in the southern branch of the arc, and the
20 other in the Cantabrian Zone foreland in the core of the arc. From this analysis it follows that the late Variscan
21 deformation together with the subsequent Alpine contraction is not sufficient to explain the formation of the Ibero-
22 Armorican Arc as a secondary structure by means of vertical axis rotations. Our analysis suggests this arc is mainly
23 a primary, or non-rotational curve, slightly modified by ca. 10% of superposed contraction during late Carboniferous
24 and/or Alpine times. Moreover, we propose that the assumptions underlying the interpreted geometry of the arc be
25 re-evaluated, and we discuss the role of late-Variscan regional strike-slip faults in the Iberian and in the Armorican
26 massifs that probably acted consecutively before and during the contraction of the arc.

27 **1. Introduction**

28 Different models have been proposed to synthesize the structural evolution and explain the characteristic arcuate
29 geometry of the western European Variscan Belt, known as the Ibero-Armorican Arc (IAA, Fig. 1). The indentor
30 model requires a curved geometry of the Gondwanan margin prior to collision and highlights the role of the
31 Gondwana promontory during the Gondwana-Laurussia collision (Matte and Ribeiro, 1975; Lefort, 1979; Brun and
32 Burg, 1982; Burg et al., 1987; Quesada, 1991; Dias and Ribeiro, 1995; Sánchez-García et al., 2003; Simancas et al.,
33 2009) (Fig. 2A). Other models propose that this arc constitutes an orocline formed by secondary vertical axis
34 buckling of an originally oriented N-S belt during Gondwana-Laurussia collision (Weil et al., 2000, 2001, 2010,
35 2013a, 2013b, 2019; Gutiérrez-Alonso et al., 2012; Fernández-Lozano et al., 2016; Pastor-Galán et al., 2011, 2012b,
36 2015a, 2017, 2019; Shaw et al., 2012) (Fig. 2B). A third group of models emphasizes the role of the large-scale
37 strike-slip shear zones and the associated deformation as the main origin for the formation of the Ibero-Armorican
38 arc (Martínez-Catalán et al., 2007; Martínez-Catalán, 2011) (Fig. 2C). Although the oroclinal and indentor models



39 may appear to be mutually exclusive, some authors reconcile both models in a proposal involving a combination of
40 some indentation and subsequent sinistral and dextral motion along shear zones on either side of the promontory
41 (Murphy et al., 2016) or subsequent buckling (Casas and Murphy, 2018) (Fig. 2D). One of the most critical points to
42 discern between the different proposals is the amount of vertical axis rotation required. The secondary orocline
43 models propose counter-clockwise vertical axis rotations ranging from 60° or 70° to 90° for the southern arm of the
44 Ibero-Armorican Arc and clockwise rotations of 25° for the northern arm (Pastor-Galán et al., 2015a, b, 2016, 2017).
45 In contrast, the amount of rotation required for some of the models involving indentation and subsequent buckling is
46 ca. 27.5° for both branches (Casas and Murphy, 2018). Although they clearly differ, these vertical axis rotations
47 each require a significant amount of contraction and extension that has yet to be quantified but which should be
48 recognizable in the surrounding regions. With the exception of the indenter model, the other models agree that the
49 vertical axis rotations occurred in late Carboniferous-Early Permian times (ca. 305-295 Ma), after the main Variscan
50 deformational events that include the emplacement of the regional allochthons. In this contribution, we estimate the
51 amount of contraction required for the different vertical axis rotations proposed for the formation of the Ibero-
52 Armorican Arc, and we compare the obtained data with deformational structures developed simultaneously. For this
53 comparison, we focus in two areas in the southern branch of the arc: (i) the parautochthon of the Galicia-Trás-os-
54 Montes Zone and the underlying autochthonous hinterland of the Central Iberian Zone in the southern branch of the
55 arc, and (ii) the Cantabrian Zone foreland in the core of the arc. Incorporation of these results into future
56 reconstructions may test the validity of the proposed models, and constrain the geometry and the origin of the arc
57 and the role of the large strike-slip faults.
58 In this contribution we follow the Marshak's (2004) terminology for curving fold-thrust belts which distinguishes
59 between rotational and non-rotational curvatures depending on whether or not segments of the belt rotated around an
60 imaginary vertical axis.

61 2. Geological setting of the Iberian Massif

62 The Iberian Massif includes several tectonically juxtaposed geological domains with important differences in their
63 stratigraphic, structural, magmatic and metamorphic evolution (Lotze, 1945; Julivert et al., 1972; Farias et al., 1987)
64 (Fig. 1). In SW Iberia, the South-Portuguese Zone (SPZ) is a tectonically imbricated Devonian to late Carboniferous
65 stratigraphic sequence, facing towards the southwest, that consists of synorogenic marine sediments with abundant
66 volcano-sedimentary components (Oliveira et al., 2019) with Laurasian affinity (Braid et al., 2011; Pérez Cáceres et
67 al., 2017; Pereira et al., 2020). The Ossa Morena Zone (OMZ) represents the northern Gondwana margin (Quesada,
68 1991; Pereira et al., 2012), composed of Neoproterozoic, Cadomian-related, synorogenic sediments unconformably
69 overlain by lower Cambrian to Lower Devonian passive-margin volcano-sedimentary sequences (Sánchez García et
70 al., 2019; Gutierrez Marco et al., 2019), which are in turn unconformably overlain by Upper Devonian to early
71 Carboniferous flysch basins (e.g. Camargo Rocha et al., 2009; Oliveira et al., 2019).
72 The boundary of the OMZ with the northern sector of the Iberian Massif is the Coimbra-Cordoba Shear Zone (e.g.
73 Pereira et al., 2008) or the Badajoz-Cordoba Shear Zone (BCSZ) (Azor et al., 1994, 2019) (Fig. 1). The northern
74 Iberian Massif can be divided in two major domains: i) The Allochthon, called Galicia-Trás-os-Montes Zone
75 (GTMZ) includes several stacked sheets; ii) the Autochthon, comprising the Central Iberian (CIZ, hinterland), West
76 Asturo-Leonese (WALZ) and the Cantabrian Zone (CZ, foreland) in the core of the Iberian-Armorican Arc (e.g.
77 Lotze, 1945; Julivert et al., 1972; Farias et al., 1987; Gutierrez Marco et al., 1990; Pérez-Estaún et al., 1988, 1990).
78 The GTMZ show increasing tectonic transport from the lowest to the highest allochthon. In the highest tectonic



79 slices, the Upper Allochthon represents a terrane that was detached from the northern Gondwanan margin during the
80 Lower Palaeozoic opening of the Rheic Ocean, accreted to southern Laurussia in the Silurian and in the Devonian
81 during Variscan collision was thrust over the Iberian margin of Gondwana (e.g. Gómez Barreiro et al., 2007;
82 Martínez Catalán et al., 2019). The Middle Allochthon is a rootless suture zone that preserves vestiges of the Rheic
83 Ocean that was consumed by subduction beneath the southern Laurussian margin (e.g. Arenas and Sánchez
84 Martínez, 2015). The Lower Allochthon represents a segment of the Gondwanan margin that was subducted and
85 incorporated by obduction into the Variscan accretionary prism (e.g. Díez Fernández et al., 2011). The lowermost
86 tectonic unit of the GTMZ, the Parautochthon (Dias da Silva et al., 2014a, 2015, 2020; González Clavijo et al.,
87 2016) also called the Schistose Domain (Farias et al., 1987) or the Parautochthonous Thrust Complex (Ribeiro et al.,
88 1990), can be divided into Upper Parautochthon, made up of a Cambrian-Silurian stratigraphic sequence comparable
89 to the CIZ (Dias da Silva et al., 2014a, 2015, 2016); and the Lower Parautochthon comprised of synorogenic early
90 Carboniferous marine strata imbricated in a piggy-back thrust sequence (Rodrigues et al., 2013; Dias da Silva et al.,
91 2015; González Clavijo et al., 2016; Martínez Catalán et al., 2016).

92 The autochthon consists of Neoproterozoic to Lower Devonian stratigraphic sequences, within which are two major
93 unconformities that record global Lower Palaeozoic extensional events related to the formation of a passive margin
94 along the northern margin of Gondwana and the opening of the Rheic Ocean (Gutierrez Marco et al., 1990; Martínez
95 Catalán et al., 1992; Dias da Silva et al., 2011; 2014b). The WALZ and CZ preserve more proximal facies than the
96 CIZ (Marcos et al., 2004).

97 The deformation history of the Iberian Massif is complex, polyphase and diachronous. Devonian deformation (ca.
98 410-370 Ma) reflects subduction-related metamorphism followed by obduction, development of detachments and
99 out-of-sequence thrusting recognized in the allochthonous complexes of the GTMZ (e.g. Gómez Barreiro et al.,
100 2007; Martínez Catalán et al., 2009). This deformation is younger in the Lower Allochthon and older in the Upper
101 Allochthon, and records the orogenic stacking and progradation of the orogenic front towards the Gondwana
102 foreland.

103 In northern Iberia, the oldest Variscan deformation and metamorphic event started in the Upper Parautochthon and
104 CIZ (365-355 Ma) and migrated into the WALZ and CZ by about 340-310 Ma (Dallmeyer et al. 1997). This D₁-M₁
105 stage was accompanied by the development of an S₁ axial planar cleavage and by chlorite to biotite zone
106 metamorphism that was synchronous with the development of a foreland basin fed by detritus derived from both the
107 accretionary prism and the peripheral bulge in the autochthon (Dias da Silva et al., 2015). Around 340 Ma
108 (Dallmeyer et al., 1997), the Upper Parautochthon was tectonically imbricated at the base of the unrooted
109 allochthonous complexes (Martínez Catalán et al., 2009) and both were tectonically transported towards present-day
110 southeast (Dias da Silva, 2014; Dias da Silva et al., 2020). The Upper Parautochthon was thrust onto its foreland
111 basin (Lower Parautochthon) (Dias da Silva et al., 2014a, 2015). This stage (C₂ after Martínez Catalán et al., 2014)
112 was responsible for the underthrusting of the underlying autochthon, leading to the regional Barrovian
113 metamorphism peak (M₁). The emplacement of the GTMZ deformed the precursor D₁ folds (C₁ after Martínez
114 Catalán et al., 2014), and caused the folding of rocks in both Parautochthon and the underlying autochthon around
115 the basal thrust-zones of the GTMZ (Ribeiro, 1974; Dias da Silva, 2014; Pastor-Galán et al., 2019; Dias da Silva et
116 al., 2020) thus forming the Central Iberian Arc according to Martínez Catalán et al. (2014) and Dias da Silva et al.
117 (2020).

118 Tectonic stacking of the GTMZ triggered synorogenic extension and adiabatic decompression (D₂-M₂) (E₁ in
119 Martínez Catalán et al., 2014 and Alcock et al., 2015). The D₂-M₂ event (340-320 Ma) is characterized by the
120 formation of extensional gneiss domes with orogen-parallel transport of the hanging-wall lithologies towards the



121 southeast (modern coordinates) (Escuder et al., 1994; Arenas and Martínez Catalán, 2013; Díez Fernández and
122 Pereira, 2016; Rubio Pascual et al., 2016). The gneiss domes developed in northern Iberia beneath the GTMZ, are
123 rooted in the autochthon (Díez Fernández et al., 2017). The D_2 - M_2 event progressed towards more continental
124 realms, affecting the WALZ at about 320-310 Ma (Martínez Catalán et al., 2003). Synchronously, the orogenic front
125 migrated further into Gondwana, with the development of the foreland thrust belt in the CZ (Pérez-Estaún et al.,
126 1988).
127 The late Variscan (ca. 315-300 Ma) in Iberia is marked by heterogeneous upright folding and transcurrent brittle-
128 ductile shear zones, under low-grade metamorphic conditions (D_3 - M_3) (Gonzalez Clavijo et al., 1993; Gutierrez-
129 Alonso et al., 2015; Díez Fernández and Pereira, 2016, 2017; Dias da Silva et al., 2018). The D_3 - M_3 folds, folds,
130 cogenetic stretching lineations and axial planar cleavages, are parallel to the orogenic trend and with the D_1 - M_1 folds
131 (Pastor-Galán et al., 2019). At the end of the D_3 , deformation became focused into a network of brittle-ductile shear
132 zones, affecting especially the margins of D_2 - M_2 gneiss dome cores and pre- to late- D_3 granitic intrusions (Fig. 1).
133 Conjugate dextral and sinistral shear zones locally steepened the previous fabrics, causing localized retrograde
134 metamorphism, and shuffled the different tectono-metamorphic domains, juxtaposing low grade and high grade
135 metamorphic rocks (e.g. Díez Fernández and Pereira, 2016; Dias da Silva et al., 2020). During this stage (307-300
136 Ma) the Porto-Tomar Shear Zone (PTSZ, Fig. 1) formed (Gutiérrez-Alonso et al., 2015) as a major dextral strike-
137 slip shear zone that, according to some authors, connects with the dextral Armorican shear zones in the Armorican
138 Massif (Martínez-Catalán et al., 2007; Martínez-Catalán, 2011, 2012) (Fig. 1).

139 3. Proposed models for the arc formation

140 The models that propose a secondary origin for the Ibero-Armorican Arc (IAA) agree that it formed at the end of the
141 D_3 deformational event (305-295 Ma, Kasimovian-Asselian) (Weil, 2006; Weil et al., 2010; Martínez-Catalán, 2012)
142 and in a geometry that resembles a vertically-plunging fold. However, they assign different mechanisms to its
143 formation (Fig. 2B and C). A group of models argue that the arc formed as a result of a lithospheric-scale buckling
144 of an initial N-S oriented linear orogen (Weil et al., 2000, 2001, 2010, 2013a, 2013b, 2019; Gutiérrez-Alonso et al.,
145 2004, 2012; Fernández-Lozano et al., 2016; Pastor-Galán et al., 2011, 2012b, 2015a, 2017, 2019; Shaw et al., 2012).
146 This buckling caused a rotation of ca. 90° of both arms of the arc, giving rise to a vertical fold with a tight geometry
147 (Fig. 2B). This model implies a 90° change in the contraction direction (from E-W to N-S) during the Variscan
148 deformation. The model has other geodynamic implications, such as the development of an important magmatic
149 event related to delamination of the thickened lithospheric root at the core of the arc (Gutiérrez-Alonso et al., 2011).
150 Structures accounting for the deformation related to these important vertical axis rotations have been described only
151 in the Cantabrian Zone, in the core of the arc, where the development of a system of radial folds simultaneously with
152 the arc formation, together with the reactivation of existing thrust sheets (Esla Unit) and the southward thrusting of
153 the Picos de Europa Unit have been proposed (Weil et al., 2000, 2001, 2013a, 2013b; Pastor-Galán et al., 2012a;
154 Merino-Tomé et al., 2009).
155 Martínez-Catalán et al. (2007) and Martínez-Catalán (2011) have suggested that the arc formed as a result of
156 symmetrical 90° rotation of existing tectonostratigraphic zones due to continental-scale dextral shear faulting
157 originated by an oblique collision. As with the previous model, this rotation resulted in an arc with tight geometry
158 (Fig. 2C). In this model, the Porto Tomar shear zone (Ribeiro et al., 1980) merges into the South Armorican shear
159 zone (Shelley and Bossière, 2002; Martínez-Catalán et al., 2007) in the Armorican Massif. These faults were
160 initially quasi-linear and significant changes in their orientation (NE-SW in the western margin of the Iberian



161 Massif, E–W in northwest Galicia and WNW–ESE in the Armorican Massif) were caused by folding during the
162 formation of the Ibero-Armorican Arc. According to Martínez-Catalán (2011) the motion of these dextral shear
163 zones during Gondwana–Laurussia convergence explains the stratigraphic similarity between the Central Armorican
164 and the Central Iberian zones and may account for the original proximity of Crozon (western Armorican Massif) and
165 Buçaco (western Portugal) (Fig. 1) which exhibit similar Ordovician stratigraphic successions (Young, 1988, 1990;
166 Robardet, 2002 and references therein). This proposal implies a southern original position for the Armorican Massif
167 either to the south or in front of the western edge of the Iberian Massif during the Ordovician, before the
168 development of the IAA (Young, 1990; Robardet, 2002). A southernmost position for the Armorican Massif during
169 the Ordovician has also been proposed to explain the distribution of the Late Ordovician (Katian) *Nicolella*
170 Community brachiopod populations by Colmenar (2015).

171 Other group of models invoke a combination of indentation and subsequent dextral and sinistral motion along shear
172 zones on either side of the promontory (Murphy et al., 2016) or subsequent buckling (Casas and Murphy, 2018).
173 Murphy et al. (2016) propose that the continental edge can have a promontory, even if the geological belts are
174 approximately-linear and the model of Casas and Murphy (2018) is based on palinspastic restoration and pre-
175 orogenic geological constraints and proposes a Gondwanan margin with an irregular pre-Variscan geometry, with
176 two E–W oriented segments linking a N–S central segment. This Gondwanan promontory was cut and offset by
177 regional strike-slip faults, and each segment was rotated ca. 27.5° about a vertical axis during late Variscan arc
178 formation (Fig. 2D). This amount of rotation has been deduced from the geometry of the South Armorican and
179 Porto-Tomar shear zones, assuming that they initially constituted the same fault system with a linear geometry (Fig.
180 2D).

181 Some authors propose the existence of a second arc in the Iberian Massif, with opposite curvature to the IAA, the
182 Central Iberian Arc (CIA) (Fig. 1). However, there is great controversy about its age of formation or even its actual
183 existence. According to Martínez-Catalán et al. (2014) and Dias da Silva et al. (2020), the CIA was a consequence
184 of the tectonic imbrication of the GTMZ onto the Iberian autochthon. This imbrication would have caused the
185 rotation of the previous structures and stratigraphy, that was tightened during the D₃ stage, synchronously with the
186 formation of the IAA. In contrast, Shaw et al. (2012, 2014), Gutierrez-Alonso *et al.* (2015) and Weil et al. (2019)
187 have proposed that the formation of IAA and CIA arcs was contemporaneous, due to oroclinal bending of a former
188 linear orogen with a N–S trend, taking place at the end of the Variscan orogeny. However, Pastor-Galán et al.
189 (2015a, 2016, 2017, 2019) have argued that the CIA is an inherited feature that supports the pre-Variscan irregular
190 geometry of the Gondwanan margin proposed by Casas and Murphy (2018). Pastor-Galán et al. (2015a) proposed
191 that it had to have formed prior to the development of the IAA, even if the CIA were a secondary arc. Dias da Silva
192 et al. (2020) added that the secondary origin of the CIA is related to the thin skinned emplacement of a lateral
193 extrusion wedge formed by the collapse of the Variscan accretionary prism in the French Massif Central at
194 approximately 360–340 Ma.

195 4. The amount of contraction required by the different proposed models

196 A simplified way to estimate the amount of contraction required to cause rotation along the vertical axis of the
197 branches of the arc is presented in Figure 3. We estimate the amount of contraction related to the different vertical
198 axis rotations, which has been proposed for the southern branch of the IAA, by comparing the initial length of a
199 segment of the arc versus the final width that separates the tip of the two branches of the arc defined by the same
200 segment (Fig. 3). In doing so, we obtain the percentage of contraction between the two arms of the arc. The



201 contraction estimate obtained depends on the original length of the previously linear orogen and on the final shape
202 (more or less tight) of the arc. Moreover, we can estimate the amount of “lost” lithosphere by comparing the initial
203 trace of the WALZ-CZ boundary versus its final trace (Figs. 4 and 5).

204 The oroclinal bending about a vertical axis of a linear orogen (Weil et al., 2000, 2001, 2010, 2013a, 2013b, 2019;
205 Gutiérrez-Alonso et al., 2012; Fernández-Lozano et al., 2016; Pastor-Galán et al., 2011, 2012b, 2015a, 2017, 2019;
206 Shaw et al., 2012) implies a rotation of ca. 90° for both branches of the arc to obtain its tight geometry (Fig. 4A).
207 After this rotation, a fragment of the linear orogen of at least 1475 km length, exhibits a final length that is
208 equivalent to the width of the vertical fold, that is 127 km. This implies a contraction of about 91% at the tip of the
209 inner part of the generated arc (Fig. 4A), and an amount of lost lithosphere around $698 \cdot 10^3 \text{ km}^2$ (Fig. 5A).

210 A similar result was obtained in the model of the secondary fold forming as a result of strike-slip faulting (Martínez-
211 Catalán et al., 2007; Martínez-Catalán, 2011). In this case, considering an initial length of ca. 1550 km and a final
212 width measured across the fold about 95 km, the amount of required contraction is about 94% and the surface of lost
213 lithosphere is around $767 \cdot 10^3 \text{ km}^2$ (Fig. 5B). Moreover, this model implies an important phase of extension in the
214 hinterland situated north of the arc. We estimate the amount of extension required to be ca. 100% (680 to 1370 km,
215 Fig. 4B), however features associated with it have not been identified.

216 The model proposed by Casas and Murphy (2018) requires a rotation of 27.5° for both branches, similar to the ca.
217 25° clockwise rotation proposed for the northern arm of the arc by Pastor-Galán et al. (2015b). If we apply the same
218 method to the geometry proposed by Casas and Murphy (2018), the amount of contraction is considerable, ca. 54%,
219 and the reduction in the surface of lithosphere, although less than in the previous models, is also significant, around
220 $36 \cdot 10^3 \text{ km}^2$ (Fig. 5C). All the previous figures on the amount of lost lithospheric surface should be considered as
221 minimum values, as the calculations of Fig 5 assumed no change in the position of the oroclinal hinge during its
222 development.

223 5. The geological data

224 To compare these estimated amounts of contraction with actual structures developed in late Variscan times, we
225 focussed our analysis in the autochthon of the CIZ, just beneath the parautochthon of the GTMZ, where D₃
226 structures are well developed (Dias da Silva, 2014), and in the Cantabrian Zone, the core of the arc, where a
227 development of radial folds (Julivert and Marcos, 1973; Weil et al., 2000, 2001, 2012, 2013; Pastor-Galán et al.,
228 2012a), the reactivation of previous thrusts (Weil et al., 2013) and the emplacement of the youngest thrust units, the
229 Cuera Unit and the Picos de Europa Province (Merino-Tomé et al., 2009) coeval with the arc formation have been
230 proposed.

231 5.1 The Parautochthon of the GTMZ and the autochthon (CIZ) beneath

232 In NW Iberia, D₃ structures affect the GTMZ (including the Parautochthon) and the tectonically underlying CIZ
233 (Fig. 6A). These D₃ structures overprint all the previous structures, including the D₁ folds that wrap around the
234 GTMZ, the main basal thrusts and detachments that limit the allochthonous domains as well as the D₂ extensional
235 detachments and M₂ isograds that bound the gneiss dome (Azor et al., 2019; Dias da Silva et al. 2020).

236 There are two types of D₃ structures: i) fan-like heterogeneous folds whose style adapted to the previous structures,
237 creating a strain shadow with convergent folds to the east and beneath the GTMZ, which acted as a rigid body
238 (Alonso and Rodríguez, 1981; Dias da Silva, 2014); and ii) conjugate dextral and sinistral transcurrent brittle-ductile
239 shear zones (e.g. González Clavijo et al., 1993; López-Plaza and López-Moro, 2004; Gutierrez Alonso et al., 2015).



240 The shear zones predominantly affect the pre- to syn- D_3 granites and the D_2 gneiss dome cores in both the CIZ and
241 GTMZ (Escuder et al., 1994; Alcock et al., 2015; Díez Fernández et al., 2017; Dias da Silva et al., 2020).
242 In the eastern rim of GTMZ (i.e. the southern limb of the IAA), the D_3 folds range in orientation from oblique to
243 orthogonal relative to the D_1 structures. The interference of D_3 folds with D_1 and D_2 folds formed type 1 and type 2
244 fold interference patterns of Ramsay and Huber (1987) (see Pastor-Galán et al., 2019; Dias da Silva et al., 2020). As
245 a consequence, the D_3 folds have variable plunges, from vertical to sub horizontal, with WNW and to ESE sense of
246 plunge and a regular WNW-ESE axial plane. D_3 folds exhibit sub-vertical axial surfaces. The axial planar
247 crenulation cleavage (S_3) shows near vertical fan-like dispersion that is more evident where a previous sub-
248 horizontal layering is present. The folding is highly heterogeneous at all scales, with sectors where there are tight
249 isoclinal folds separated by areas with more open folds (Dias da Silva et al., 2020).
250 Retrograde metamorphism and the reworking of the previous fabrics occur adjacent to brittle-ductile transcurrent
251 conjugate shear zones. These shear zones also produce proto-mylonitic to ultra-mylonitic fabrics associated with
252 faults, with intrafolial and sheath folds, C- and C'-S pairs, quarter structures, tectonic fish and sigmoidal shapes in
253 porphyroclasts and syn-tectonic porphyroblasts (as in the aureoles of the syn- to late- D_3 granites) (Dias da Silva et
254 al., 2020). However, in upper structural levels, these features are less common. Instead, a well developed crenulation
255 cleavage is associated with tight isoclinal folds. Taken together, it appears that D_3 flattening was accommodated by
256 motion along conjugate transcurrent shear zones in the high grade metamorphic domains (gneiss domes, granites,
257 etc.) and by folding in the low grade metamorphic domains (Dias da Silva et al., 2020).
258 The D_3 folds and shear zones enclose pre-to syn- D_3 granitic bodies, which acted as rigid bodies. The D_3 structures
259 steepened some pre-existing structures, such as the thrusts and detachments of the GTMZ and the D_2 - M_2 fabrics and
260 isograds of the gneiss domes (e.g. Díez-Fernández and Pereira, 2016, 2017; Dias da Silva et al., 2020). The regional
261 orientation of D_3 structures changes from N-S in the western limb of the IAA to WNW-ESE in the southern limb of
262 the IAA (Martínez Catalán et al., 2014).
263 The value of contraction caused by the D_3 structures in the CIZ was estimated from a cross-section (Fig. 6B). The
264 base of the Armorican Quartzite was chosen to calculate the contraction in two sectors not affected by granite
265 intrusions (Fig. 6C). Adding both sectors and comparing their initial and final lengths, the elongation obtained was
266 equal to -0.05, implying a contraction (horizontal shortening) of 5%. However, the additional contraction produced
267 by the conjugate, upright, transcurrent brittle-ductile shear zones should be included, although clear markers cannot
268 be identified to get an estimation, and no significant displacement of the granitic batholiths is depicted in Fig. 6B.

269 5.2 The Cantabrian Zone

270 The Cantabrian Zone (CZ) is the external thrust-and-fold belt of the Variscan orogen that developed by thin-skinned
271 deformation at the end of the Carboniferous (Julivert, 1971; Marcos and Pulgar, 1982; Perez-Estaún et al., 1988).
272 The thrust-and-fold belt deforms pre-orogenic and syn-orogenic Paleozoic sedimentary successions. The youngest
273 strata of the pre-orogenic succession are Lower Carboniferous in age and form a sedimentary wedge thinning
274 towards the foreland. The syn-orogenic succession includes late Carboniferous strata and occurs as several clastic
275 wedges that were deposited in foredeeps coeval with the major thrust events (Marcos and Pulgar, 1982).
276 The CZ includes a set of arcuate thrust units that were emplaced from west to east in present coordinates. The oldest
277 thrusts are in the SW and are Bashkirian (Westphalian A) in age (Arbolea, 1981; Marcos and Pulgar, 1982),
278 whereas the youngest are in the east and are latest Moscovian to Gzhelian in age (Merino-Tomé et al., 2009). The
279 thrust units include frontal fault-bend and fault-propagation folds developed in response to the ramp-and-flat



280 geometry of corresponding thrusts (i.e. Bastida et al., 1984; Alonso, 1987; Pérez-Estaún et al., 1988; Alvarez-
281 Marron, 1995; Bulnes and Aller, 2002; among others) (Fig. 7, 8). The major folds in the CZ have been classified
282 into two sets based on the distribution of axial traces in map view with respect to the trend of major thrusts that
283 impart the arcuate shape to the CZ (Julivert and Marcos, 1973). Folds with axial traces trending sub-parallel to the
284 trace of the thrusts, mostly developed within individual thrust-sheets, have been classified as longitudinal folds,
285 whereas folds with axial traces trending sub-perpendicular to the thrusts that extend across several major thrust units
286 have been classified as radial folds.

287 More recent studies have shown that lateral structures in the form of ramps and folds and tear faults are common.
288 These lateral structures may have developed in individual thrust sheets or may reflect the complex evolution and
289 superposition during emplacement of the thrust pile. The large tectonic superposition of some of the thrust units also
290 caused accommodation structures in the form of lateral culminations and drop faults on a previously emplaced thrust
291 sheet above an active underlying sheet. In the CZ, a change in the direction of tectonic transport is particularly
292 evident between the emplacement of the Picos de Europa and Ponga Units. The former shows transport towards the
293 NE and E (Alvarez-Marrón, 1995) whereas the latter shows transport towards the S and SSW (Marquínez, 1989).

294 Most individual thrust-related folds were modified during progressive thrusting and almost every major fold had a
295 distinctive evolution during the development of the Cantabrian Zone thrust systems. As a result, most folds
296 originally classified as longitudinal folds are now considered as frontal thrust-related folds (Alonso, 1987, Perez-
297 Estaún et al., 1988) (Fig. 8) and some folds classified as radial folds are now considered as lateral thrust-related
298 folds (Alonso, 1987; Bastida and Castro, 1988; Alvarez-Marron, 1995). The Ponga Unit provides a good example of
299 the variety in distribution, dimensions and attitude of thrust-related folds in the CZ (Fig. 7). The Ponga Unit lies in
300 the core of the CZ and shows a complex fold interference pattern that was mainly caused by the superposition of
301 thrust units with different emplacement directions. The emplacement direction was northeastward in rear thrust
302 sheets but eastward in the frontal thrusts. Most lateral folds with E-W orientation were tightened during the
303 subsequent south-directed emplacement of the Picos de Europa Unit (Alvarez-Marron, 1995).

304 The timing of formation of thrust-related folds in the CZ, spans the whole time of development of the Cantabrian
305 Thrust Systems. The emplacement of earliest thrust units (Somiedo-Correcilla and Esla Units; Arboleya, 1981)
306 occurred in the late Bashkirian (~ 318 Ma). The south to south-southwest emplacement of the frontal unit in the
307 internal part of the arc (Picos de Europa Province) occurred during the Kasimovan-Ghezelian transition (~ 304 Ma)
308 (Merino-Tomé et al., 2009). According to these authors the emplacement of the Picos de Europa Province caused
309 contraction of 150 ± 15 km that was distributed between southward displacement of the Cuera-Picos de Europa
310 imbricate thrust system, reactivation of previous thrusts and out-of-sequence thrusting, and by internal deformation.
311 Part of this contraction also may account for the tightening of the previously formed E-W oriented lateral folds in
312 the Ponga Unit (Alvarez-Marron, 1995).

313 Further evidence for the age of formation of longitudinal and radial folds in the CZ is provided by structures
314 associated with a Late-Variscan extensional episode and metamorphism (Valin et al., 2016). This episode includes
315 the development of a cleavage that crosscuts longitudinal and radial folds and the frontal thrust of the Picos de
316 Europa Unit (Aller et al., 1987; Aller et al., 2005; Valin et al., 2016). This cleavage is associated with very low to
317 low grade metamorphism (Bastida et al., 1999; García-Lopez et al, 2018), and is overprinted by contact
318 metamorphic aureoles related to granodiorites emplacement at $292 \pm 2/- 3$ Ma (Valverde-Vaquero et al., 1999).

319 6. Discussion



320 **6.1 The geometry of the IAA**

321 Most models for the IAA agree that the arc has a very tight geometry (Fig. 1). This interpretation assumes: 1) the
322 correlation of stratigraphy of the northern limb of the arc across the Bay of Biscay, and 2) eastward continuation of
323 the northern arm of the arc across NE Iberia. However, both assumptions are problematic.

324 1) The correlation across the northern arm across the Bay of Biscay is speculative due to poor exposure, and thus
325 strongly depends on the location attributed to the Iberian Plate in Late Permian–Early Jurassic times. However the
326 Mesozoic evolution of the Iberian Plate is controversial. Different interpretations of the Mesozoic Atlantic and Bay
327 of Biscay magnetic anomalies, especially magnetic anomalies older than M0 chron (ca. 125 Ma), have yielded
328 several end-member models for the reconstruction of the Iberian Plate motion with different initial positions (see
329 Barnett-Moore et al. 2016 and Muñoz 2019 for a detailed discussion) (Fig. 9). This is a critical uncertainty as the
330 position and orientation of the Iberian Plate at the end of the Variscan orogeny strongly constrains the geometry of
331 the Ibero-Armorican Arc. Until the extent of rotation due to Alpine orogenesis is understood, the problem of lateral
332 correlation involving the megastructures on both sides of the Bay of Biscay renders any reconstruction of the Ibero-
333 Armorican Arc highly speculative.

334 2) The geometry of the southwestern arm of the Ibero-Armorican Arc is tightly constrained by correlations of the
335 Cambrian-Ordovician sequences within WALZ and Ollo de Sapo magmatic rocks within the CIZ (Montero et al.,
336 2007; Montero et al., 2009, among others), both of which can be traced for hundreds of kilometres along strike
337 (Martínez-Catalán et al., 2007). However, the geometry of the eastern arm of the arc is not so well constrained. This
338 eastern branch would include the Basque massif or sub-domain (western Pyrenees) and the south-westernmost inlier
339 of the Coastal Catalanian Ranges (Priorat massif), which are thought to represent the lateral continuation of the
340 West Asturian-Leonese Zone (Martínez-Catalán et al., 2007) (Fig. 1). In the same way, the remainder of the
341 Pyrenees is thought to be equivalent to the CIZ (Martínez-Catalán et al., 2007) (Fig. 1). However, as widely
342 documented, the Cambrian–Ordovician geodynamic, stratigraphic and zircon provenance evolution of the eastern
343 Pyrenees fits better with other neighbouring areas, such as the Montagne Noire and southern Sardinia, than with the
344 rest of the Iberian Massif (see discussion in Álvaro et al., 2018; Casas et al., 2019). As a result, the northern and
345 eastern prolongations of the Ibero-Armorican Arc are not well defined, compromising interpretations of the
346 proposed tight geometry of the arc.

347 **6.2 The origin of the arc**

348 The analysis of the D₃ structures affecting the autochthon of the GTMZ provided shortening values of about 5-10%
349 (Fig. 6). This value is far less than the estimated 91%-94% of contraction required to form IAA as a secondary
350 orocline, as proposed in the oroclinal and strike-slip models (Weil et al., 2000, 2001, 2010, 2013a, 2013b, 2019;
351 Gutiérrez-Alonso et al., 2012; Fernández-Lozano et al., 2016; Pastor-Galán et al., 2011, 2012b, 2015a, 2017, 2019;
352 Shaw et al., 2012; Martínez-Catalán et al. 2007; Martínez-Catalán, 2011). It is also significantly less than the 54%
353 contraction implied in the model involving indentation and subsequent buckling (Casas and Murphy 2018).

354 In the CZ core of the arc, the horizontal contraction of 150±15 km related to the emplacement of Picos de Europa
355 Unit (Merino-Tomé et al., 2009) must be re-evaluated. Using the control points proposed by these authors (Fig. 11,
356 Merino-Tomé et al., 2009), the contraction related to the emplacement of the imbricate thrust system is around 58
357 km. These 58 km represent only one third of the approximate contraction of 164 km experienced by this segment of
358 the Cantabrian Zone if it developed as a result of the bending around a vertical axis of a linear orogen (see insert in
359 Fig. 4A). In addition, the age of emplacement of these youngest thrust units in the Cantabrian zone towards the



360 south is documented to have been ongoing from 304 to 299 Ma (Valin et al., 2016; Merino-Tomé et al., 2009),
361 coetaneous with the sedimentation of the molasses, Kasimovian to Gzhelian in age (Merino-Tomé et al., 2009,
362 2019-Fig. 11.5). In turn, these molasses unconformably overlie NW-SE and W-E-oriented thrusts and folds in the
363 southern Cantabrian Zone (e.g. in the Villablino coalfield, which cross-cuts the WALZ-CZ boundary (IGME, 1982),
364 and the La Magdalena coalfield (IGME, 1984). That is, these strata postdate not only the emplacement of the major
365 tectonic units in the CZ but also the arc formation, which must be older than the emplacement of the Picos de
366 Europa Unit. Moreover, the CIZ-WALZ boundary should had experienced a contraction of 109 km (32%), in a N-S
367 direction, during the closure of the arc (see insert in Fig. 4A), whereas no structures attributable to this have been
368 reported inside the WALZ.

369 Additionally, we propose that N-S contraction during the development of the Alpine deformation along the northern
370 Iberian margin may also have contributed to some tightening of the arc. In the southern border of the CZ, Marín et
371 al. (1995) estimated 20 km of contraction in Domo de Valsurvio and Curavacas syncline during the Alpine
372 deformation. Pulgar et al. (1999) have proposed a similar South displacement of ca. 22 km for the entire CZ. This
373 moderate Alpine overprinting of Variscan features is similar to that described in other areas of the Iberian Massif.
374 For example, Alpine thrusts caused displacements ranging between 25 to 30 km in the Iberian Range (Casas-Sáinz,
375 1993; Guimerà et al., 1995), and ca. 25 km in the Central System (Warburton and Álvarez, 1989). An Alpine
376 contraction of 40 km to 60 km in a NNE-SSW direction has been estimated for the whole Iberian Range (Guimerà et
377 al., 1995, 2004; Guimerà, 2018). The superposition of Alpine over Variscan folds has also been proposed in the
378 Carboniferous rocks of the Priorat area in the Catalan Coastal Range (Valenzuela et al., 2016).

379 Even considering late Variscan deformation in combination with Alpine deformation there is not enough contraction
380 to explain the formation of the arc as a secondary structure. The results of our analysis suggest the Ibero-Armorican
381 Arc is mainly a primary or non-rotational curvature, slightly modified during late Carboniferous and Alpine times.
382 This model implies that the relationship between the Central Iberian Arc and the Ibero-Armorican Arc, considered
383 both as margin-controlled curves, remains an open question.

384 **6.3 The role of the large strike-slip faults**

385 In the models involving strike-slip faulting deformation and oblique collision (Martínez-Catalán et al., 2007;
386 Martínez-Catalán, 2011) or indentation and subsequent buckling (Casas and Murphy, 2018), the large late-Variscan
387 dextral strike-slip faults play an important role (Fig. 2C and D). In both cases it has been assumed that the Porto
388 Tomar shear zone merges in the Armorican Massif with the South Armorican shear zones (Fig. 1) and that these
389 shear zones were initially linear. It is also assumed that they constitute the southern margin of the French Massif
390 Central. Using Crozon (Brittany) and Buçaco (Portugal) areas as piercing points, Casas and Murphy (2018)
391 estimated a total dextral offset of around 900 km between the Iberian and Armorican massifs during the late
392 Moscovian-Kasimovian along the Porto Tomar-South Armorican shear zone system, before its folding during the
393 arc deformation. However, if a primary origin for the arc is assumed, another relationship between these strike-slip
394 faults must be envisaged, as the South Armorican and the Porto Tomar shear zone system would not represent the
395 same megastructure before the arc formation. An alternative explanation is to consider that they constitute two
396 separate faults that acted consecutively. First, a dextral displacement along the NE-SW Porto Tomar shear zone of
397 about 450 km, and then offset of this structure by the dextral movement of the South Armorican shear zone system
398 oriented WNW-ESE. In this case, the northern prolongation of the Porto Tomar shear zone may be located
399 somewhere in the Northern Armorican Domain. The restoration of this strike-slip faults consecutive movement



400 results in a pre-tectonic arrangement of the different tectono-stratigraphic units compatible with the paleogeographic
401 reconstruction proposed by Casas and Murphy (2018).

402 7. Conclusions

403 From the analysis proposed here, it follows that late Variscan deformation together with the Alpine deformation is
404 not sufficient to explain the formation of Ibero-Armorican Arc as a secondary structure by means of vertical axis
405 rotations. We propose that this arc is mainly a primary, or non-rotational curve, slightly modified by ca. 10% of
406 superposed contraction during late Carboniferous and/or Alpine times.

407 Therefore, this amount of deduced contraction cannot account for the tight curvature of the Ibero-Armorican Arc if
408 originated as a linear orogenic feature. Moreover, the North side of this curvature is not supported by regional
409 geological data. We consider it necessary to re-evaluate the geometry of the arc, after considering how Alpine
410 movements affected the post-Variscan position of the Iberian Plate.

411 Another relationship between the late-Variscan large strike-slip faults in the Iberian and in the Armorican massifs
412 must be envisaged. Probably the Porto Tomar and the South Armorican shear zone systems do not represent the
413 same megastructure on both sides of the Bay of Biscay. Instead, these structures may have acted consecutively.

414 Acknowledgements

415 We acknowledge the financial support provided by CGL2017-87631-P, CGL2016-76438-P, PGC2018-093903-B-
416 C22 and SALTCONBELT-CGL2017- 85532-P projects, funded by Agencia Estatal de Investigación (AEI) and
417 Fondo Europeo de Desarrollo Regional (FEDER); and by project 2014SGR-467 (GEOMODELS Research Institute
418 and the Grup de Geodinàmica i Anàlisi de Conques). IDS thanks the financial support given by the “Estímulo ao
419 Emprego Científico – Norma Transitória” national science contract in the Faculdade de Ciências da Universidade de
420 Lisboa. This work is a contribution to the IGCP project 648, the IDL’s Research Group 3 (Solid Earth dynamics,
421 hazards and resources) and to IDL’s FCT-projects FCT/UID/GEO/50019/2019-IDL and FCT/UIDB/50019/2020-
422 IDL. Detailed revision by J.B. Murphy greatly improved a first version of this manuscript.

423 References

- 424 Alcock, J. E., Martínez Catalán, J. R., Rubio Pascual, F. J., Díez Montes, A., Díez Fernández, R., Gómez Barreiro,
425 J., Arenas, R., Dias da Silva, Í., and González-Clavijo, E.: 2-D thermal modeling of HT-LP metamorphism in NW
426 and Central Iberia: Implications for Variscan magmatism, rheology of the lithosphere and orogenic evolution,
427 *Tectonophysics*, 657, 21-37, doi: 10.1016/j.tecto.2015.05.022, 2015
- 428 Alonso, J. L.: Sequences of thrusts and displacement transfer in the superposed duplexes of the Esla Nappe Region
429 (cantabrian zone, nw spain), *Journal of Structural Geology*, 9, 969-983, doi: [https://doi.org/10.1016/0191-](https://doi.org/10.1016/0191-8141(87)90005-8)
430 [8141\(87\)90005-8](https://doi.org/10.1016/0191-8141(87)90005-8), 1987
- 431 Alonso, J. L. and Rodríguez Fernández, L. R.: Aportaciones al conocimiento de la estructura del Sinclinorio de
432 Verin, *Cuadernos Xeolóxicos de Laxe*, 1981. 93-122, 1981
- 433 Alvarez-Marron, J.: Three-dimensional geometry and interference of fault-bend folds: examples from the Ponga
434 Unit, Variscan Belt, NW Spain, *Journal of Structural Geology*, 17, 549-560, doi: [https://doi.org/10.1016/0191-](https://doi.org/10.1016/0191-8141(94)00075-B)
435 [8141\(94\)00075-B](https://doi.org/10.1016/0191-8141(94)00075-B), 1995



- 436 Álvaro, J. J., Casas, J. M., Clausen, S., and Quesada, C.: Early Palaeozoic geodynamics in NW Gondwana, *Journal*
437 *of Iberian Geology*, 44, 551-565, doi: 10.1007/s41513-018-0079-x, 2018
- 438 Aller, J., Bastida, F., Brime, C., and Perez-Estaun, A.: Cleavage and its relation with metamorphic grade in the
439 Cantabrian Zone (Hercynian of North-West Spain), *Sciences Géologiques, bulletins et mémoires*, 255-272, doi:
440 10.3406/sgeol.1987.1765, 1987
- 441 Aller, J., Valín, M. a. L., García-López, S., Brime, C., and Bastida, F.: Superposition of tectono-thermal episodes in
442 the southern Cantabrian Zone (foreland thrust and fold belt of the Iberian Variscides, NW Spain), *Bulletin de la*
443 *Société Géologique de France*, 176, 487-497, doi: 10.2113/176.6.487, 2005
- 444 Arboleya, M. L.: La estructura del Manto del Esla (Cordillera Cantábrica, León), *Boletín geológico y minero*, 1981.
445 19-40, 1981
- 446 Arenas, R. and Martínez Catalán, J. R.: Low-P metamorphism following a Barrovian-type evolution. Complex
447 tectonic controls for a common transition, as deduced in the Mondoñedo thrust sheet (NW Iberian Massif),
448 *Tectonophysics*, 365, 143-164, doi: 10.1016/S0040-1951(03)00020-9, 2003
- 449 Arenas, R. and Sanchez-Martinez, S.: Variscan ophiolites in NW Iberia: Tracking lost Paleozoic oceans and the
450 assembly of Pangea, *Episodes*, 38, 315-333, doi: 10.18814/epiugs/2015/v38i4/82427, 2015
- 451 Azor, A., Dias da Silva, Í., Gómez Barreiro, J., González-Clavijo, E., Martínez Catalán, J. R., Simancas, J. F.,
452 Martínez Poyatos, D., Pérez-Cáceres, I., González Lodeiro, F., Expósito, I., Casas, J. M., Clariana, P., García-
453 Sansegundo, J., and Margalef, A.: Deformation and Structure. In: *The Geology of Iberia: A Geodynamic Approach:*
454 *Volume 2: The Variscan Cycle*, Quesada, C. and Oliveira, J. T. (Eds.), Springer International Publishing, Cham, doi:
455 10.1007/978-3-030-10519-8_10, 2019
- 456 Azor, A., Lodeiro, F. G., and Simancas, J. F.: Tectonic evolution of the boundary between the Central Iberian and
457 Ossa-Morena zones (Variscan belt, southwest Spain), *Tectonics*, 13, 45-61, doi: 10.1029/93TC02724, 1994
- 458 Barnett-Moore, N., Hosseinpour, M., and Maus, S.: Assessing discrepancies between previous plate kinematic
459 models of Mesozoic Iberia and their constraints, *Tectonics*, 35, 1843-1862, doi: 10.1002/2015TC004019, 2016
- 460 Bastida, F., Brime, C., García-López, S., and Sarmiento, G. N.: Tectono-thermal evolution in a region with thin-
461 skinned tectonics: the western nappes in the Cantabrian Zone (Variscan belt of NW Spain), *International Journal of*
462 *Earth Sciences*, 88, 38-48, doi: 10.1007/s005310050244, 1999
- 463 Bastida, F. and Castro, S.: Estructura del sector septentrional de la Escama de Tamiza (Zona Cantábrica, NW de
464 España), *Trabajos de geología*, 17, 67-87, 1988
- 465 Bastida, F., Marcos, A., Pérez-Estaún, A., and Pulgar, J.: Geometría y evolución estructural del Manto de Somiedo
466 (Zona Cantábrica, NO de España), *Boletín Geológico y Minero*, 95, 3-25, 1984
- 467 Braid, J. A., Murphy, J. B., Quesada, C., and Mortensen, J.: Tectonic escape of a crustal fragment during the closure
468 of the Rheic Ocean: U–Pb detrital zircon data from the Late Palaeozoic Pulo do Lobo and South Portuguese zones,
469 southern Iberia, *Journal of the Geological Society*, 383-392, doi: 10.1144/0016-76492010-104, 168, 2011
- 470 Brun, J. P. and Burg, J. P.: Combined thrusting and wrenching in the Ibero-Armorican arc: A corner effect during
471 continental collision, *Earth and Planetary Science Letters*, 61, 319-332, 1982, doi: 10.1016/0012-821X(82)90063-2,
472 1982
- 473 Bulnes, M. and Aller, J.: Three-dimensional geometry of large-scale fault-propagation folds in the Cantabrian Zone,
474 NW Iberian Peninsula, *Journal of Structural Geology*, 24, 827-846, doi: https://doi.org/10.1016/S0191-
475 8141(01)00114-6, 2002



- 476 Burg, J. P., Bale, P., Brun, J.-P., and Girardeau, J.: Stretching lineation and transport direction in the Ibero-
477 Armorican arc during the siluro-devonian collision, *Geodinamica Acta*, 1, 71-87, doi:
478 10.1080/09853111.1987.11105126, 1987
- 479 Camargo Rocha, R., Ventura Araújo, A. A., Santos Borrego, J., and Fonseca, P. E.: Transected folds with opposite
480 patterns in Terena Formation (Ossa Morena Zone, Portugal): anomalous structures resulting from sedimentary basin
481 anisotropies, *Geodinamica Acta*, 22, 157-163, doi: 10.3166/ga.22.157-163, 2009
- 482 Casas, J. M., Álvaro, J. J., Clausen, S., Padel, M., Puddu, C., Sanz-López, J., Sánchez-García, T., Navidad, M.,
483 Castiñeiras, P., and Liesa, M.: Palaeozoic Basement of the Pyrenees. In: *The Geology of Iberia: A Geodynamic*
484 *Approach: Volume 2: The Variscan Cycle*, Quesada, C. and Oliveira, J. T. (Eds.), Springer International Publishing,
485 Cham, doi: 10.1007/978-3-030-10519-8_8, 2019
- 486 Casas, J. M. and Murphy, J. B.: Unfolding the arc: The use of pre-orogenic constraints to assess the evolution of the
487 Variscan belt in Western Europe, *Tectonophysics*, 736, 47-61, doi: <https://doi.org/10.1016/j.tecto.2018.04.012>, 2018
- 488 Casas Sainz, A. M.: Oblique tectonic inversion and basement thrusting in the Cameros Massif (Northern Spain),
489 *Geodinamica Acta*, 6, 202-216, doi: 10.1080/09853111.1993.11105248, 1993
- 490 Colmenar, J.: The arrival of brachiopods of the Nicolella Community to the Mediterranean margin of Gondwana
491 during the Late Ordovician: Palaeogeographical and palaeoecological implications, *Palaeogeography,*
492 *Palaeoclimatology, Palaeoecology*, 428, 12-20, doi: <https://doi.org/10.1016/j.palaeo.2015.03.030>, 2015
- 493 Dallmeyer, R. D., Martínez Catalán, J. R., Arenas, R., Gil Ibarguchi, J. I., Gutiérrez-Alonso, G., Farias, P., Bastida,
494 F., and Aller, J.: Diachronous Variscan tectonothermal activity in the NW Iberia Massif: Evidence from 40Ar/39Ar
495 dating of regional fabrics, *Tectonophysics*, 277, 307-337, doi: 10.1016/S0040-1951(97)00035-8, 1997
- 496 Dias da Silva, Í.: *Geología de las Zonas Centro Ibérica y Galicia – Trás-os-Montes en la parte oriental del Complejo*
497 *de Morais, Portugal/España*, Instituto Universitario de Geología "Isidro Parga Pondal" - Área de Xeoloxía e Minería
498 do Seminario de Estudos Galegos, Coruña, 2014.
- 499 Dias da Silva, Í., González Clavijo, E., Barba, P., Valladares, M. I., and Ugidos, J. M.: Geochemistry of Lower
500 Palaeozoic shales. A case study in a sector of the Iberian Variscides. In: *Ordovician of the World - 11th*
501 *International Symposium on the Ordovician System*, Gutiérrez Marco, J. C., Rábano, I., and García-Bellido, D.
502 (Eds.), Instituto Geológico y Minero de España, Alcalá de Henares, 2011
- 503 Dias da Silva, Í., Jensen, S., and González Clavijo, E.: Trace fossils from the Desejosa Formation (Schist and
504 Greywacke Complex, Douro Group, NE Portugal): new Cambrian age constraints, *Geologica Acta*, 12, 109-120,
505 doi: 10.1344/105.000002080, 2014a
- 506 Dias da Silva, Í., Valverde-Vaquero, P., González-Clavijo, E., Díez-Montes, A., and Martínez Catalán, J. R.:
507 Structural and stratigraphical significance of U–Pb ages from the Mora and Saldanha volcanic complexes (NE
508 Portugal, Iberian Variscides), *Geological Society, London, Special Publications*, 405, 115-135, doi:
509 10.1144/sp405.3, 2014b
- 510 Dias da Silva, Í., Linnemann, U., Hofmann, M., González-Clavijo, E., Díez-Montes, A., and Martínez Catalán, J. R.:
511 Detrital zircon and tectonostratigraphy of the Parautochthon under the Morais Complex (NE Portugal): implications
512 for the Variscan accretionary history of the Iberian Massif, *Journal of the Geological Society*, 172, 45-61, doi:
513 10.1144/jgs2014-005, 2015
- 514 Dias da Silva, Í., Díez Fernández, R., Díez-Montes, A., González Clavijo, E., and Foster, D. A.: Magmatic evolution
515 in the N-Gondwana margin related to the opening of the Rheic Ocean—evidence from the Upper Parautochthon of
516 the Galicia-Trás-os-Montes Zone and from the Central Iberian Zone (NW Iberian Massif), *International Journal of*
517 *Earth Sciences*, 105, 1127-1151, doi: 10.1007/s00531-015-1232-9, 2016



- 518 Dias da Silva, Í., Pereira, M. F., Silva, J. B., and Gama, C.: Time-space distribution of silicic plutonism in a gneiss
519 dome of the Iberian Variscan Belt: The Évora Massif (Ossa-Morena Zone, Portugal), *Tectonophysics*, 747-748, 298-
520 317, doi: 10.1016/j.tecto.2018.10.015, 2018
- 521 Dias da Silva, Í., González Clavijo, E., and Díez-Montes, A.: The collapse of the Variscan belt: a Variscan lateral
522 extrusion thin-skinned structure in NW Iberia, *International Geology Review*, 1-37, doi:
523 10.1080/00206814.2020.1719544, 2020
- 524 Dias, R. and Ribeiro, A.: The Ibero-Armorican Arc: A collision effect against an irregular continent?,
525 *Tectonophysics*, 246, 113-128, doi: 10.1016/0040-1951(94)00253-6, 1995
- 526 Díez Fernández, R. and Pereira, M. F.: Strike-slip shear zones of the Iberian Massif: Are they coeval?, *Lithosphere*,
527 9, 726-744, doi: 10.1130/L648.1, 2017
- 528 Díez Fernández, R., Martínez Catalán, J. R., Arenas Martín, R., and Abati Gómez, J.: Tectonic evolution of a
529 continental subduction-exhumation channel: Variscan structure of the basal allochthonous units in NW Spain,
530 *Tectonics*, 30, 1-22, doi: 10.1029/2010TC002850, 2011
- 531 Díez Fernández, R., Parra, L. M. M., and Rubio Pascual, F. J.: Extensional flow produces recumbent folds in syn-
532 orogenic granitoids (Padrón migmatitic dome, NW Iberian Massif), *Tectonophysics*, 703-704, 69-84, doi:
533 10.1016/j.tecto.2017.03.010, 2017
- 534 Díez Fernández, R. and Pereira, M. F.: Extensional orogenic collapse captured by strike-slip tectonics: Constraints
535 from structural geology and UPb geochronology of the Pinhel shear zone (Variscan orogen, Iberian Massif),
536 *Tectonophysics*, 691, 290-310, doi: 10.1016/j.tecto.2016.10.023, 2016
- 537 Escuder Viruete, J., Arenas, R., and Martínez Catalán, J. R.: Tectonothermal evolution associated with Variscan
538 crustal extension, in the Tormes Gneiss dome (NW Salamanca, Iberian Massif, Spain), *Tectonophysics*, 238, 1-22,
539 doi: 10.1016/0040-1951(94)90052-3, 1994
- 540 Farias, P., Gallastegui, G., González-Lodeiro, F., Marquínez, J., Martín Parra, L. M., Martínez Catalán, J. R., de
541 Pablo Maciá, J. G., and Rodríguez Fernández, L. R.: Aportaciones al conocimiento de la litoestratigrafía y estructura
542 de Galicia Central, *Memórias da Faculdade de Ciências da Universidade do Porto*, 1, 411-431, 1987
- 543 Fernández-Lozano, J., Pastor-Galán, D., Gutiérrez-Alonso, G., and Franco, P.: New kinematic constraints on the
544 Cantabrian orocline: A paleomagnetic study from the Peñalba and Truchas synclines, NW Spain, *Tectonophysics*,
545 681, 195-208, doi: <https://doi.org/10.1016/j.tecto.2016.02.019>, 2016
- 546 García-López, S., Voldman, G. G., Bastida, F., and Aller, J.: Tectonothermal analysis of a major unit of the
547 Cantabrian Zone: the Ponga unit (Variscan belt, NW Spain), *International Journal of Earth Sciences*, 107, 2727-
548 2740, doi: 10.1007/s00531-018-1623-9, 2018
- 549 Gómez Barreiro, J., Martínez Catalán, J. R., Arenas, R., Castiñeiras, P., Abati, J., Díaz García, F., and Wijbrans, J.
550 R.: Tectonic evolution of the upper allochthon of the Órdenes complex (Northwestern Iberian Massif): Structural
551 constraints to a polygenic peri-Gondwanan terrane, *Geologic Society of America - Special paper*, 423, 315-332, doi:
552 10.1130/2007.2423(15), 2007
- 553 González Clavijo, E., Díez Balda, M. A., and Álvarez, F.: Structural study of a semiductile strike-slip system in the
554 Central Iberian Zone (Variscan Fold Belt, Spain): Structural controls on gold deposits, *Geologische Rundschau*, 82,
555 448-460, doi: 10.1007/BF00212409, 1993
- 556 González Clavijo, E., Dias da Silva, Í. F., Gutiérrez-Alonso, G., and Díez Montes, A.: U/Pb age of a large dacitic
557 block locked in an Early Carboniferous synorogenic mélangé in the Parautochthon of NW Iberia: New insights on
558 the structure/sedimentation Variscan interplay, *Tectonophysics*, 681, 159-169, doi: 10.1016/j.tecto.2016.01.001,
559 2016



- 560 Guimerà, J.: Structure of an intraplate fold-and-thrust belt: The Iberian Chain. *Geologica acta*, 16,
561 0427-0438, doi: 10.1344/GeologicaActa2018.16.4.6., 2018
- 562 Guimerà, J., Alonso, Á., and Mas, J. R.: Inversion of an extensional-ramp basin by a newly formed thrust: the
563 Cameros basin (N. Spain), *Geological Society, London, Special Publications*, 88, 433, doi:
564 10.1144/GSL.SP.1995.088.01.23, 1995
- 565 Guimerà, J., Mas, R., and Alonso, A.: Intraplate deformation in the NW Iberian Chain: Mesozoic extension and
566 Tertiary contractional inversion, *Journal of the Geological Society*, 161, 291-303, doi: 10.1144/0016-764903-055,
567 2004
- 568 Gutiérrez-Alonso, G., Fernández-Suárez, J., and Weil, A. B.: Orocline triggered lithospheric delamination, *Geologic
569 Society of America - Special paper*, 383, 121-130, doi: 10.1130/0-8137-2383-3(2004) 383[121:OTLD] 2.0.CO;2,
570 2004
- 571 Gutiérrez-Alonso, G., Fernández-Suárez, J., Jeffries, T. E., Johnston, S. T., Pastor-Galán, D., Murphy, J. B., Franco,
572 P., and Gonzalo, J. C.: Diachronous post-orogenic magmatism within a developing orocline in Iberia, *European
573 Variscides, Tectonics*, 30, 17, doi: 10.1029/2010TC002845, 2011
- 574 Gutiérrez-Alonso, G., Johnston, S., Weil, A., Pastor-Galán, D., and Fernández-Suárez, J.: Buckling an orogen: the
575 Cantabrian Orocline, *GSA Today*, 22, 4-9, doi: 10.1130/GSATG141A.1, 2012
- 576 Gutiérrez-Alonso, G., Collins, A. S., Fernández-Suárez, J., Pastor-Galán, D., González-Clavijo, E., Jourdan, F.,
577 Weil, A. B., and Johnston, S. T.: Dating of lithospheric buckling: $40\text{Ar}/39\text{Ar}$ ages of syn-orocline strike-slip shear
578 zones in northwestern Iberia, *Tectonophysics*, 643, 44-54, doi: 10.1016/j.tecto.2014.12.009, 2015
- 579 Gutiérrez-Marco, J. C., San José, M. A., and Pieren, A. P.: Post-Cambrian Paleozoic stratigraphy. In: *Pre-Mesozoic
580 Geology of Iberia*, Dallmeyer, R. D. and Martínez García, E. (Eds.), Springer-Verlag, Germany, 1990
- 581 Gutiérrez-Marco, J. C., Piçarra, J. M., Meireles, C. A., Cózar, P., García-Bellido, D. C., Pereira, Z., Vaz, N., Pereira,
582 S., Lopes, G., Oliveira, J. T., Quesada, C., Zamora, S., Esteve, J., Colmenar, J., Bernárdez, E., Coronado, I.,
583 Lorenzo, S., Sá, A. A., Dias da Silva, Í., González-Clavijo, E., Díez-Montes, A., and Gómez-Barreiro, J.: Early
584 Ordovician–Devonian Passive Margin Stage in the Gondwanan Units of the Iberian Massif. In: *The Geology of
585 Iberia: A Geodynamic Approach: Volume 2: The Variscan Cycle*, Quesada, C. and Oliveira, J. T. (Eds.), Springer
586 International Publishing, Cham, doi: 10.1007/978-3-030-10519-8_3, 2019
- 587 Jammes, S., Manatschal, G., Lavier, L., and Masini, E.: Tectosedimentary evolution related to extreme crustal
588 thinning ahead of a propagating ocean: Example of the western Pyrenees, *Tectonics*, 28, doi:
589 10.1029/2008TC002406, 2009
- 590 Julivert, M.: Decollement tectonics in the Hercynian Cordillera of Northwest Spain, *American Journal of Science*,
591 270, 1-29, doi: 10.2475/ajs.270.1.1, 1971
- 592 Julivert, M., Fonboté, J. M., Ribeiro, A., and Conde, L.: Memoria explicativa del Mapa Tectónico de la Península
593 Ibérica y Baleares. Escala 1:1.000.000, Instituto Geológico y Minero de España, Madrid, 1972.
- 594 Julivert, M. and Marcos, A.: Superimposed folding under flexural conditions in the Cantabrian Zone (Hercynian
595 Cordillera, northwest Spain), *American Journal of Science*, 273, 353-375, doi: 10.2475/ajs.273.5.353, 1973
- 596 Lefort, J. P.: Iberian-Armorican arc and Hercynian orogeny in western Europe, *Geology*, 7, 384-388, doi:
597 10.1130/0091-7613(1979)7<384:iaahoi>2.0.co;2, 1979
- 598 López-Plaza, M. and López-Moro, F. J.: El Domo del Tormes. In: *Geología de España*, Vera, J. A. (Ed.), SGE-
599 IGME, Madrid, 2004
- 600 Lotze, F.: Observaciones respecto de la división de los Variscides de la Meseta Ibérica, *Publ. Extr. Geol. España*, V
601 (1950), 145-167, 1945



- 602 I.G.M.E.: Mapa geológico de España, 1:50 000. No 101 (Villablino). Servicio de Publicaciones del Ministerio de
603 Industria y Energía, Madrid, Mem. 56p.,
604 (<http://info.igme.es/cartografiadigital/geologica/Magna50Hoja.aspx?intranet=false&id=101>), 1982
- 605 I.G.M.E.: Mapa geológico de España, 1:50 000. No 129 (La Robla). Servicio de Publicaciones del Ministerio de
606 Industria y Energía, Madrid, Mem. 98p.
607 (<http://info.igme.es/cartografiadigital/geologica/Magna50Hoja.aspx?intranet=false&id=129>), 1984
- 608 Marcos, A., Martínez Catalán, J. R., Gutiérrez Marco, J. C., and Pérez-Estaún, A.: Estratigrafía y paleogeografía. In:
609 Geología de España, Vera, J. A. (Ed.), SGE-IGME, Madrid, 2004
- 610 Marcos, A. and Pulgar, J.: An approach to the tectonostratigraphic evolution of the Cantabrian foreland thrust and
611 fold belt, Hercynian Cordillera of NW Spain, Neues Jahrbuch fuer Geologie und Palaeontologie. Abhandlungen,
612 163, 256-260, 1982
- 613 Marín, J., Pulgar, J., and Alonso, J.: La deformación alpina en el Domo de Valsurvio (Zona Cantábrica, NO de
614 España), Revista de la Sociedad Geológica de España, 8, 111-116, 1995
- 615 Marquínez, J.: Mapa geológico de la Región del Cuera y los Picos de Europa, Trabajos de Geología, 18, 137-144,
616 1989
- 617 Marshak, S.: Salients, recesses, arcs, Oroclines, and Syntaxes - A review of ideas concerning the formation of map-
618 view curves in fold-thrust belts, AAPG Memoir, 82, 131-144, 2004
- 619 Martínez Catalán, J. R.: Are the oroclines of the Variscan belt related to late Variscan strike-slip tectonics?, Terra
620 Nova, 23, 241-247, doi: 10.1111/j.1365-3121.2011.01005.x, 2011
- 621 Martínez Catalán, J. R.: The Central Iberian arc, an orocline centered in the Iberian Massif and some implications
622 for the Variscan belt, International Journal of Earth Sciences, 101, 1299-1314, doi: 10.1007/s00531-011-0715-6,
623 2012
- 624 Martínez Catalán, J. R., Hacer Rodriguez, M. P., Villar Alonso, P., Perez-Estaún, A., and Gonzalez Lodeiro, F.:
625 Lower Paleozoic extensional tectonics in the limit between the West Asturian-Leonese and Central Iberian Zones of
626 the Variscan Fold-Belt in NW Spain, Geologische Rundschau, 81, 545-560, doi: 10.1007/bf01828614, 1992
- 627 Martínez Catalán, J. R., Arenas, R., and Díez Balda, M. A.: Large extensional structures developed during the
628 emplacement of a crystalline thrust sheet: the Mondoñedo nappe (NW Spain), Journal of Structural Geology, 25,
629 1815-1839, doi: 10.1016/S0191-8141(03)00038-5, 2003
- 630 Martínez Catalán, J. R., Arenas, R., Díaz García, F., González Cuadra, P., Gómez Barreiro, J., Abati, J., Castiñeiras,
631 P., Fernández-Suárez, J., Sánchez Martínez, S., Andonaegui, P., González Clavijo, E., Díez Montes, A., Rubio
632 Pascual, F., and Valle Aguado, B.: Space and time in the tectonic evolution of the northwestern Iberian Massif:
633 Implications for the Variscan belt. In: 4-D Framework of Continental Crust, Hatcher Jr., R. D., Carlson, M. P.,
634 McBride, J. H., and Martínez Catalán, J. R. (Eds.), Geologic Society of America, Boulder, doi:
635 10.1130/2007.1200(21), 2007
- 636 Martínez Catalán, J. R., Arenas, R., Abati, J., Sánchez Martínez, S., Díaz García, F., Fernández-Suárez, J., González
637 Cuadra, P., Castiñeiras, P., Gómez Barreiro, J., Díez Montes, A., González Clavijo, E., Rubio Pascual, F.,
638 Andonaegui, P., Jeffries, T. E., Alcock, J. E., Díez Fernández, R., and López Carmona, A.: A rootless suture and the
639 loss of the roots of a mountain chain: The Variscan Belt of NW Iberia, C.R. Geoscience, 341, 114-126, doi:
640 10.1016/j.erte.2008.11.004, 2009
- 641 Martínez Catalán, J. R., Rubio Pascual, F. J., Montes, A. D., Fernández, R. D., Barreiro, J. G., Dias Da Silva, Í.,
642 Clavijo, E. G., Ayarza, P., and Alcock, J. E.: The late Variscan HT/LP metamorphic event in NW and Central



- 643 Iberia: relationships to crustal thickening, extension, orocline development and crustal evolution, Geological
644 Society, London, Special Publications, 405, 225-247, doi: 10.1144/sp405.1, 2014
- 645 Martínez Catalán, J. R., González Clavijo, E., Meireles, C., Díez Fernández, R., and Bevis, J.: Relationships
646 between syn-orogenic sedimentation and nappe emplacement in the hinterland of the Variscan belt in NW Iberia
647 deduced from detrital zircons, Geological Magazine, 153, 38-60, doi: 10.1017/S001675681500028X, 2016
- 648 Martínez Catalán, J. R., Gómez Barreiro, J., Dias da Silva, Í., Chichorro, M., López-Carmona, A., Castiñeiras, P.,
649 Abati, J., Andonaegui, P., Fernández-Suárez, J., González Cuadra, P., and Benítez-Pérez, J. M.: Variscan Suture
650 Zone and Suspect Terranes in the NW Iberian Massif: Allochthonous Complexes of the Galicia-Trás os Montes
651 Zone (NW Iberia). In: The Geology of Iberia: A Geodynamic Approach: Volume 2: The Variscan Cycle, Quesada,
652 C. and Oliveira, J. T. (Eds.), Springer International Publishing, Cham, doi: 10.1007/978-3-030-10519-8_4, 2019
- 653 Matte, P. and Ribeiro, A.: Forme et orientation de l'ellipsoïde de déformation dans la vibration Hercynienne de
654 Galicie: relation avec le plissement et hypothèses sur la genèse de l'arc Iberio-Armoricain, Comptes Rendus de
655 l'Académie des Sciences, 1975. 2825-2828, 1975
- 656 Merino-Tomé, O. A., Bahamonde, J. R., Colmenero, J. R., Heredia, N., Villa, E., and Farias, P.: Emplacement of the
657 Cuera and Picos de Europa imbricate system at the core of the Iberian-Armorican arc (Cantabrian zone, north
658 Spain): New precisions concerning the timing of arc closure, GSA Bulletin, 121, 729-751, doi: 10.1130/B26366.1,
659 2009
- 660 Merino-Tomé, O., Alonso, J. L., Bahamonde, J.R., Marcos, A., Colmenero, J.R., Villa, E., and Suárez, A.: Foreland
661 Basin at the Cantabrian Zone: Evolution from the Distal Foreland Basin Successions to Wedge-Top Deposition and
662 the Tightening of the Ibero-Armorican Arc. In: The Geology of Iberia: A Geodynamic Approach: Volume 2: The
663 Variscan Cycle, Quesada, C. and Oliveira, J. T. (Eds.), Springer International Publishing, Cham, doi: 10.1007/978-
664 3-030-10519-8_10, 2019
- 665 Montero, P., Bea, F., González Lodeiro, F., Talavera, C., and Whitehouse, M. J.: Zircon ages of the metavolcanic
666 rocks and metagranites of the Ollo de Sapo Domain in central Spain: implications for the Neoproterozoic to Early
667 Palaeozoic evolution of Iberia, Geological Magazine, 144, 963-976, doi: 10.1017/S0016756807003858, 2007
- 668 Montero, P., Bea, F., Corretgé, L. G., Floor, P., and Whitehouse, M. J.: U-Pb ion microprobe dating and Sr and Nd
669 isotope geology of the Galíñeiro Igneous Complex: A model for the peraluminous/peralkaline duality of the
670 Cambro-Ordovician magmatism of Iberia, Lithos, 107, 227-238, doi: 10.1016/j.lithos.2008.10.009, 2009
- 671 Muñoz, J. A.: Alpine Orogeny: Deformation and Structure in the Northern Iberian Margin (Pyrenees s.l.). In: The
672 Geology of Iberia: A Geodynamic Approach: Volume 3: The Alpine Cycle, Quesada, C. and Oliveira, J. T. (Eds.),
673 Springer International Publishing, Cham, doi: 10.1007/978-3-030-11295-0_9, 2019
- 674 Murphy, J. B., Quesada, C., Gutiérrez-Alonso, G., Johnston, S. T., and Weil, A.: Reconciling competing models for
675 the tectono-stratigraphic zonation of the Variscan orogen in Western Europe, Tectonophysics, 681, 209-219, doi:
676 <http://dx.doi.org/10.1016/j.tecto.2016.01.006>, 2016
- 677 Oliveira, J. T., González-Clavijo, E., Alonso, J., Armendáriz, M., Bahamonde, J. R., Braid, J. A., Colmenero, J. R.,
678 Dias da Silva, Í., Fernandes, P., Fernández, L. P., Gabaldón, V., Jorge, R. S., Machado, G., Marcos, A., Merino-
679 Tomé, Ó., Moreira, N., Murphy, J. B., Pinto de Jesus, A., Quesada, C., Rodrigues, B., Rosales, I., Sanz-López, J.,
680 Suárez, A., Villa, E., Piçarra, J. M., and Pereira, Z.: Synorogenic Basins. In: The Geology of Iberia: A Geodynamic
681 Approach: Volume 2: The Variscan Cycle, Quesada, C. and Oliveira, J. T. (Eds.), Springer International Publishing,
682 Cham, doi: 10.1007/978-3-030-10519-8_11, 2019
- 683 Pastor-Galán, D., Gutiérrez-Alonso, G., and Weil, A. B.: Orocline timing through joint analysis: Insights from the
684 Ibero-Armorican Arc, Tectonophysics, 507, 31-46, doi: 10.1016/j.tecto.2011.05.005, 2011



- 685 Pastor-Galán, D., Gutiérrez-Alonso, G., Mulchrone, K. F., and Huerta, P.: Conical folding in the core of an orocline.
686 A geometric analysis from the Cantabrian Arc (Variscan Belt of NW Iberia), *Journal of Structural Geology*, 39, 210-
687 223, doi: <https://doi.org/10.1016/j.jsg.2012.02.010>, 2012a
- 688 Pastor-Galán, D., Gutiérrez-Alonso, G., Zulauf, G., and Zanella, F.: Analogue modeling of lithospheric-scale
689 orocline buckling: Constraints on the evolution of the Iberian-Armorican Arc, *GSA Bulletin*, 124, 1293-1309, doi:
690 10.1130/B30640.1, 2012b
- 691 Pastor-Galán, D., Groenewegen, T., Brouwer, D., Krijgsman, W., and Dekkers, M. J.: One or two oroclines in the
692 Variscan orogen of Iberia? Implications for Pangea amalgamation, *Geology*, 43, 527-530, doi: 10.1130/g36701.1,
693 2015a
- 694 Pastor-Galán, D., Ursem, B., Meere, P. A., and Langereis, C.: Extending the Cantabrian Orocline to two continents
695 (from Gondwana to Laurussia). Paleomagnetism from South Ireland, *Earth and Planetary Science Letters*, 432, 223-
696 231, doi: 10.1016/j.epsl.2015.10.019, 2015b
- 697 Pastor-Galán, D., Dekkers, M. J., Gutiérrez-Alonso, G., Brouwer, D., Groenewegen, T., Krijgsman, W., Fernández-
698 Lozano, J., Yenes, M., and Álvarez-Lobato, F.: Paleomagnetism of the Central Iberian curve's putative hinge: Too
699 many oroclines in the Iberian Variscides, *Gondwana Research*, 39, 96-113, doi: 10.1016/j.gr.2016.06.016, 2016
- 700 Pastor-Galán, D., Gutiérrez-Alonso, G., Dekkers, M. J., and Langereis, C. G.: Paleomagnetism in Extremadura
701 (Central Iberian zone, Spain) Paleozoic rocks: extensive remagnetizations and further constraints on the extent of the
702 Cantabrian orocline, *Journal of Iberian Geology*, doi: 10.1007/s41513-017-0039-x, 2017
- 703 Pastor-Galán, D., Dias da Silva, Í. F., Groenewegen, T., and Krijgsman, W.: Tangled up in folds: tectonic
704 significance of superimposed folding at the core of the Central Iberian curve (West Iberia), *International Geology*
705 *Review*, 61, 240-255, doi: 10.1080/00206814.2017.1422443, 2019
- 706 Pereira, M. F., Chichorro, M., Silva, J. B., Ordóñez-Casado, B., Lee, J. K. W., and Williams, I. S.: Early
707 carboniferous wrenching, exhumation of high-grade metamorphic rocks and basin instability in SW Iberia:
708 Constraints derived from structural geology and U–Pb and 40Ar–39Ar geochronology, *Tectonophysics*, 558–559,
709 28-44, doi: <http://dx.doi.org/10.1016/j.tecto.2012.06.020>, 2012
- 710 Pereira, M. F., Gama, C., Dias da Silva, Í., Fuenlabrada, J. M., Silva, J. B., and Medina, J.: Isotope geochemistry
711 evidence for Laurussian-type sources of South-Portuguese Zone Carboniferous turbidites (Variscan orogeny),
712 *Geological Society, London, Special Publications*, 503, SP503-2019-2163, doi: 10.1144/sp503-2019-163, 2020
- 713 Pérez-Cáceres, I., Martínez Poyatos, D., Simancas, J. F., and Azor, A.: Testing the Avalonian affinity of the South
714 Portuguese Zone and the Neoproterozoic evolution of SW Iberia through detrital zircon populations, *Gondwana*
715 *Research*, 42, 177-192, doi: <https://doi.org/10.1016/j.gr.2016.10.010>, 2017
- 716 Pérez-Estaún, A., Bastida, F., Alonso, J. L., Marquínez, J., Aller, J., Alvarez-Marrón, J., Marcos, A., and Pulgar, J.
717 A.: A thin-skinned tectonics model for an arcuate fold and thrust belt: The Cantabrian Zone (Variscan Ibero-
718 Armorican Arc), *Tectonics*, 7, 517-537, doi: 10.1029/TC007i003p00517, 1988
- 719 Pérez-Estaún, A., Bastida, F., Martínez Catalán, J. R., Gutierrez Marco, J. C., Marcos, A., and Pulgar, J. A.: West
720 Asturian-Leonese Zone. Stratigraphy. In: *Pre-Mesozoic Geology of Iberia*, Dallmeyer, R. D. and Martínez García,
721 E. (Eds.), Springer-Verlag, Berlin, 1990
- 722 Pulgar, J., Alonso, J., Espina, R., and Marín, J.: La deformación alpina en el basamento varisco de la Zona
723 Cantábrica, *Trabajos de geología*, 21, 283-295, 1999
- 724 Quesada, C.: Geological constraints on the Paleozoic tectonic evolution of tectonostratigraphic terranes in the
725 Iberian Massif, *Tectonophysics*, 185, 225-245, doi: 10.1016/0040-1951(91)90446-Y, 1991



- 726 Ribeiro, A. (Ed.): Contribution à l'étude tectonique de Trás-os-Montes Oriental, Serviços Geológicos de Portugal,
727 Lisboa, 1974.
- 728 Ribeiro, A., Pereira, E., and Severo, L.: Análise da deformação da zona de cisalhamento Porto-Tomar na transversal
729 de Oliveira de Azeméis, Comunicações dos Serviços Geológicos de Portugal, 66, 3-9, 1980
- 730 Ribeiro, A., Pereira, E., Dias, R., Gil Iburguchi, J. I., and Arenas, R.: Allochthonous Sequences. In: Pre-Mesozoic
731 Geology of Iberia, Dallmeyer, R. D. and Garcia, E. M. (Eds.), Springer Berlin Heidelberg, Berlin, Heidelberg, doi:
732 10.1007/978-3-642-83980-1_15, 1990
- 733 Robardet, M.: Alternative approach to the Variscan Belt in southwestern Europe: Preorogenic paleobiogeographical
734 constraints. In: Variscan-Appalachian dynamics: The building of the late Paleozoic basement, Catalán, J. R. M.,
735 Hatcher, R. D., Jr., Arenas, R., and García, F. D. (Eds.), Geological Society of America, doi: 10.1130/0-8137-2364-
736 7.1, 2002
- 737 Rodrigues, J. F., Ribeiro, A., and Pereira, E.: Complexo de Mantos Parautóctones do NE de Portugal: estrutura
738 interna e tectonoestratigrafia. In: Geologia de Portugal, Dias, R., Araújo, A., Terrinha, P., and Kullberg, J. C. (Eds.),
739 Escolar Editora, Lisboa, 2013
- 740 Rubio Pascual, F. J., López-Carmona, A., and Arenas, R.: Thickening vs. extension in the Variscan belt: P–T
741 modelling in the Central Iberian autochthon, Tectonophysics, 681, 144-158, doi: 10.1016/j.tecto.2016.02.033, 2016
- 742 Sánchez-García, T., Bellido, F., and Quesada, C.: Geodynamic setting and geochemical signatures of Cambrian–
743 Ordovician rift-related igneous rocks (Ossa-Morena Zone, SW Iberia), Tectonophysics, 365, 233-255, doi:
744 https://doi.org/10.1016/S0040-1951(03)00024-6, 2003
- 745 Sánchez-García, T., Chichorro, M., Solá, A. R., Álvaro, J. J., Díez-Montes, A., Bellido, F., Ribeiro, M. L., Quesada,
746 C., Lopes, J. C., Dias da Silva, Í., González-Clavijo, E., Gómez Barreiro, J., and López-Carmona, A.: The
747 Cambrian-Early Ordovician Rift Stage in the Gondwanan Units of the Iberian Massif. In: The Geology of Iberia: A
748 Geodynamic Approach: Volume 2: The Variscan Cycle, Quesada, C. and Oliveira, J. T. (Eds.), Springer
749 International Publishing, Cham, doi: 10.1007/978-3-030-10519-8_2, 2019
- 750 Shaw, J., Johnston, S. T., Gutiérrez-Alonso, G., and Weil, A. B.: Oroclines of the Variscan orogen of Iberia:
751 Paleocurrent analysis and paleogeographic implications, Earth and Planetary Science Letters, 329-330, 60-70, doi:
752 10.1016/j.epsl.2012.02.014, 2012
- 753 Shaw, J., Gutiérrez-Alonso, G., Johnston, S. T., and Pastor Galán, D.: Provenance variability along the Early
754 Ordovician north Gondwana margin: Paleogeographic and tectonic implications of U-Pb detrital zircon ages from
755 the Armorican Quartzite of the Iberian Variscan belt, Geological Society of America Bulletin, doi:
756 10.1130/b30935.1, 2014
- 757 Shelley, D. and Bossière, G. r.: Megadisplacements and the Hercynian orogen of Gondwanan France and Iberia. In:
758 Variscan-Appalachian dynamics: The building of the late Paleozoic basement, Catalán, J. R. M., Hatcher, R. D., Jr.,
759 Arenas, R., and García, F. D. (Eds.), Geological Society of America, doi: 10.1130/0-8137-2364-7.209, 2002
- 760 Simancas, J. F., Azor, A., Martínez-Poyatos, D., Tahiri, A., El Hadi, H., González-Lodeiro, F., Pérez-Estaún, A.,
761 and Carbonell, R.: Tectonic relationships of Southwest Iberia with the allochthons of Northwest Iberia and the
762 Moroccan Variscides, Comptes Rendus Geoscience, 341, 103-113, doi: 10.1016/j.crte.2008.11.003, 2009
- 763 Srivastava, S. P., Sibuet, J. C., Cande, S., Roest, W. R., and Reid, I. D.: Magnetic evidence for slow seafloor
764 spreading during the formation of the Newfoundland and Iberian margins, Earth and Planetary Science Letters, 182,
765 61-76, doi: 10.1016/S0012-821X(00)00231-4, 2000



- 766 Valín, M. L., García-López, S., Brime, C., Bastida, F., and Aller, J.: Tectonothermal evolution in the core of an
767 arcuate fold and thrust belt: the south-eastern sector of the Cantabrian Zone (Variscan belt, north-western Spain),
768 *Solid Earth*, 7, 1003-1022, doi: 10.5194/se-7-1003-2016, 2016
- 769 Valverde-Vaquero, P., Cuesta, A., Gallastegui, G., Suárez, O., Corretgé, L., and Dunning, G.: U-Pb dating of late
770 Variscan magmatism in the Cantabrian Zone (Northern Spain), *Terra Abstracts*, 101, 1999.
- 771 Vallenzuela, S., Alias, G., and Casas, J. M.: Superposition relations of microfabrics in the northern hanging-wall
772 block of the Évora Massif (Ossa-Morena Zone), IX Congreso Geológico de España (Geotemas 16), Huelva, 109-
773 112, 2016.
- 774 Warburton, J. and Alvarez, C.: A thrust tectonic interpretation of the Guadarrama Mountains, Spanish Central
775 System. Libro homenaje a Rafael Soler, Asociación de Geólogos y Geofísicos Españoles del Petróleo, 1989
- 776 Weil, A. B., Van der Voo, R., van der Pluijm, B. A., and Parés, J. M.: The formation of an orocline by multiphase
777 deformation: a paleomagnetic investigation of the Cantabria–Asturias Arc (northern Spain), *Journal of Structural*
778 *Geology*, 22, 735-756, doi: 10.1016/S0191-8141(99)00188-1, 2000
- 779 Weil, A. B., Van der Voo, R., and Van der Pluijm, B. A.: Oroclinal bending and evidence against the Pangea
780 megashear: The Cantabria-Asturias arc (northern Spain), *Geology*, 29, 991-994, doi: 10.1130/0091-
781 7613(2001)029<0991:OBAEAT>2.0.CO;2, 2001
- 782 Weil, A. B.: Kinematics of orocline tightening in the core of an arc: Paleomagnetic analysis of the Ponga Unit,
783 Cantabrian Arc, northern Spain, *Tectonics*, 25, doi: 10.1029/2005tc001861, 2006
- 784 Weil, A. B., Gutiérrez-Alonso, G., and Conan, J.: New time constraints on lithospheric-scale oroclinal bending of
785 the Ibero-Armorican Arc: a palaeomagnetic study of earliest Permian rocks from Iberia, *Journal of the Geological*
786 *Society*, 167, 127-145, doi: 10.1144/0016-76492009-002, 2010
- 787 Weil, A. B., Gutiérrez-Alonso, G., Johnston, S. T., and Pastor-Galán, D.: Kinematic constraints on buckling a
788 lithospheric-scale orocline along the northern margin of Gondwana: A geologic synthesis, *Tectonophysics*, 582, 25-
789 49, doi: 10.1016/j.tecto.2012.10.006, 2013a
- 790 Weil, A. B., Gutiérrez-Alonso, G., and Wicks, D.: Investigating the kinematics of local thrust sheet rotation in the
791 limb of an orocline: a paleomagnetic and structural analysis of the Esla tectonic unit, Cantabrian–Asturian Arc, NW
792 Iberia, *International Journal of Earth Sciences*, 102, 43-60, doi: 10.1007/s00531-012-0790-3, 2013b
- 793 Weil, A., Pastor-Galán, D., Johnston, S. T., and Gutiérrez-Alonso, G.: Late/Post Variscan Orocline Formation and
794 Widespread Magmatism. In: *The Geology of Iberia: A Geodynamic Approach: Volume 2: The Variscan Cycle*,
795 Quesada, C. and Oliveira, J. T. (Eds.), Springer International Publishing, Cham, doi: 10.1007/978-3-030-10519-
796 8_14, 2019
- 797 Young, T. P.: The lithostratigraphy of the upper Ordovician of central Portugal, *Journal of the Geological Society*,
798 145, 377-392, doi: 10.1144/gsjgs.145.3.0377, 1988
- 799 Young, T. P.: Ordovician sedimentary facies and faunas of southwest Europe: palaeogeographic and tectonic
800 implications, *Geological Society, London, Memoirs*, 12, 421, doi: 10.1144/GSL.MEM.1990.012.01.39, 1990
- 801



802 **FIGURE CAPTIONS**

803 **Fig. 1.** Map of the Variscan belt of Western and Central Europe at post-Variscan times (ca. 295 Ma, Early Permian)
804 with the location of the different areas and structures referred to in the text, after Martínez-Catalán (2011) modified.
805 Abbreviations: B (Buçaco); BCSZ (Badajoz-Córdoba shear zone); C (Crozon); CO (Corsica); CIZ (Central Iberian
806 Zone); CZ (Cantabrian Zone); ECM (External crystalline massif of the Alps); FMC (French Massif Central); GTMZ
807 (Galicia Tras-Os-Montes Zone); JPSZ (Juzbado-Peñalba shear zone); LC (Lizard Complex); LLF (Layale-Lubine
808 fault); LT (Leon terrane shear zone); MAD (Mid Armorican Domain); MDZ (Moldanubian Zone); MM (Maures
809 Massif); MS (Moravo-Silesian Unit); NAD (North Armorican Domain); NASZ (North Armorican shear zone); NEF
810 (Nort-sur Erdre fault); OMZ (Ossa Morena Zone); PY (Pyrenees); PTSZ (Porto-Tomar shear zone); RHZ (Rhen
811 Hercynian Zone); SA (Sardinia); SAD (Southern Armorican Domain); SAF (Southern Armorican front); SASZ
812 (South Armorican shear zone, N and S: northern and southern branches); SISZ (Southern Iberia shear zone); SPZ
813 (South Portuguese Zone); SXZ (Saxo-Thuringian Zone); TBZ (Teplá-Barrandian Zone); VF (Variscan Front); VM
814 (Vosges Massif); WALZ (West Asturian Leonese Zone). See text for explanation.

815 **Fig. 2.** Various models for the formation of the Ibero-Armorican Arc. A) Indentor model after Sánchez-García et al.
816 (2003). B) Oroclinal bending about a vertical axis after Pastor-Galán et al. (2017). C) Dextral mega-shear model
817 from Martínez-Catalán et al. (2007). D) Combination of margin-controlled and buckling from Casas and Murphy
818 (2018).

819 **Fig. 3.** Contraction related to 90° rotations of both arms of an initially linear orogen with different initial lengths.

820 **Fig. 4.** Contraction related to: A) oroclinal bending about a vertical axis of an initial linear orogeny (after Pastor-
821 Galán et al., 2017 modified); B) lithospheric bending as a response to strike-slip faulting (after Martínez-Catalán et
822 al., 2007 modified); C) arc formed as a result of combination of margin-controlled curve and buckling (after Casas
823 and Murphy, 2018 modified).

824 **Fig. 5.** Estimation of the amount of lost lithosphere related to: A) oroclinal bending about a vertical axis of an initial
825 linear orogeny (after Pastor-Galán et al., 2017 modified); B) lithospheric bending as a response to strike-slip faulting
826 (after Martínez-Catalán et al., 2007 modified); C) arc formed as a result of combination of margin-controlled curve
827 and buckling (after Casas and Murphy, 2018 modified).

828 **Fig. 6.** A) Simplified geological map of the eastern rim of the Morais Allochthonous Complex (Galicia-Trás-os-
829 Montes Zone) and the underlying parautochthonous and autochthonous domains, showing the main Variscan
830 structures and the location of the cross section in B. This area is located in the axial zone of the Central Iberian Arc
831 (CIA). B) Cross section cutting the axial zone of the CIA showing the horizontal shortening related to the D₃
832 structures in the autochthon of the CIZ, underlying the GTMZ. The contraction produced by D₃ folds at the base of
833 the Armorican Quartzite (red thick lines) is measured in two sectors. Modified after Dias da Silva (2014) and Dias
834 da Silva et al. (2020). Abbreviations: BLPD - Basal Lower Parautochthon Detachment; MTMT - Main Trás-os-
835 Montes Thrust. For location, see Fig. 1.

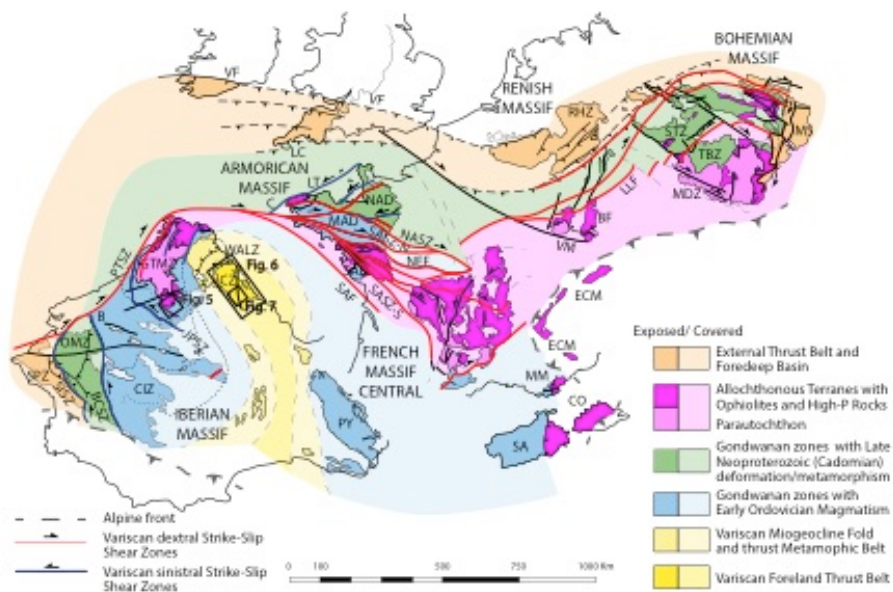
836 **Fig. 7.** A) Geological map of the Ponga Unit that is at the core of the Cantabrian Zone arc, from Alvarez-Marrón
837 (1995) (location in the inset). B) Axial traces of folds grouped into three sets frontal, corner, and lateral folds by
838 Alvarez-Marrón (1995). The fault-bend folds have varied dimensions and orientations depending on the dimensions
839 and orientations of the ramps and flats of the thrusts. Corner folds form oblique to the other two sets, at the
840 intersection of lateral and frontal ramps. The interference and tectonic superposition of lateral and frontal thrust



841 structures cause the plunge of fold axis (see Alvarez-Marron, 1995 for the classification of the different types of fold
842 interactions). Frontal folds plunges are in the direction perpendicular to the transport direction. Lateral folds over
843 frontal ramps plunges are in the direction of the tectonic transport. For location, see Fig. 1.

844 **Fig. 8.** A) Distribution of footwall ramps and flats in the Ponga Unit basal thrust is shown as an example of how
845 large folds such as Rio Color Antiform and Rio Monasterio Antiforms are related to the lateral footwall ramps of the
846 basal thrust. Arrows indicate the emplacement direction of different thrust units mostly based on field kinematic
847 indicators (Alvarez-Marrón, 1995). B) Geological cross-section that illustrated the geometries of large E-W folds, the
848 thrust stacking and the lateral ramps in the footwall to the basal thrust (location in 7A). C) Block diagramme
849 showing the ideal geometry of the basal thrust of the Ponga Unit (Alvarez-Marrón, 1995). For location, see Fig. 1.

850 **Fig. 9.** End-member plate models reconstructions of the Iberian Plate relative to a fixed Eurasia at chron M0. A)
851 Taken from Srivastava et al. (2000); B) From Jammes et al. (2009), after Barnett-Moore et al. (2016) modified. Red
852 lines: Variscan dextral strike-slip faults, blue lines: Variscan sinistral strike-slip faults. Latitudes, in degrees, refer to
853 their present position in France.
854

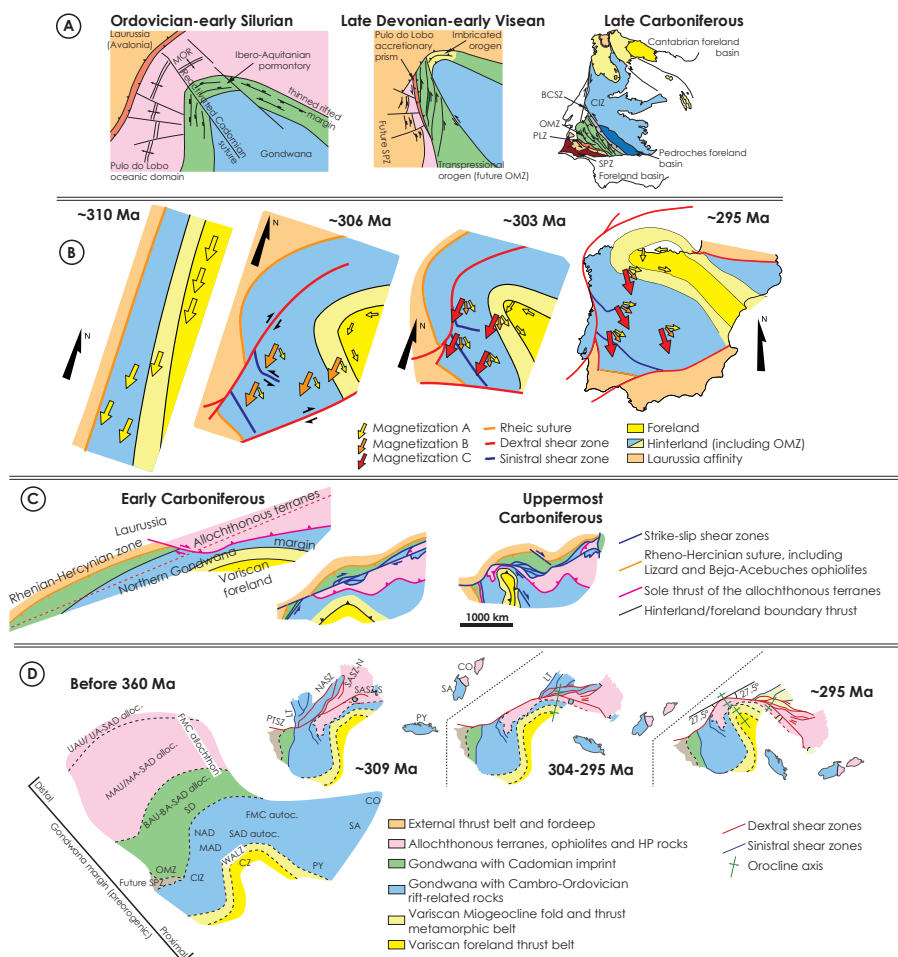


855

856

857 Fig. 1.

858

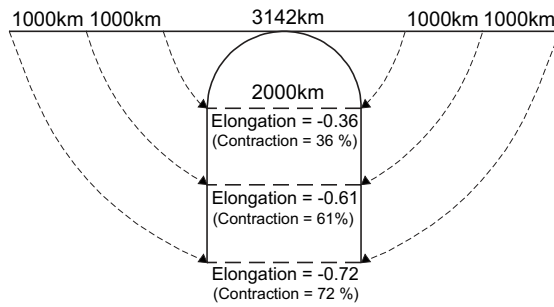


859

860

861 Fig. 2.

862

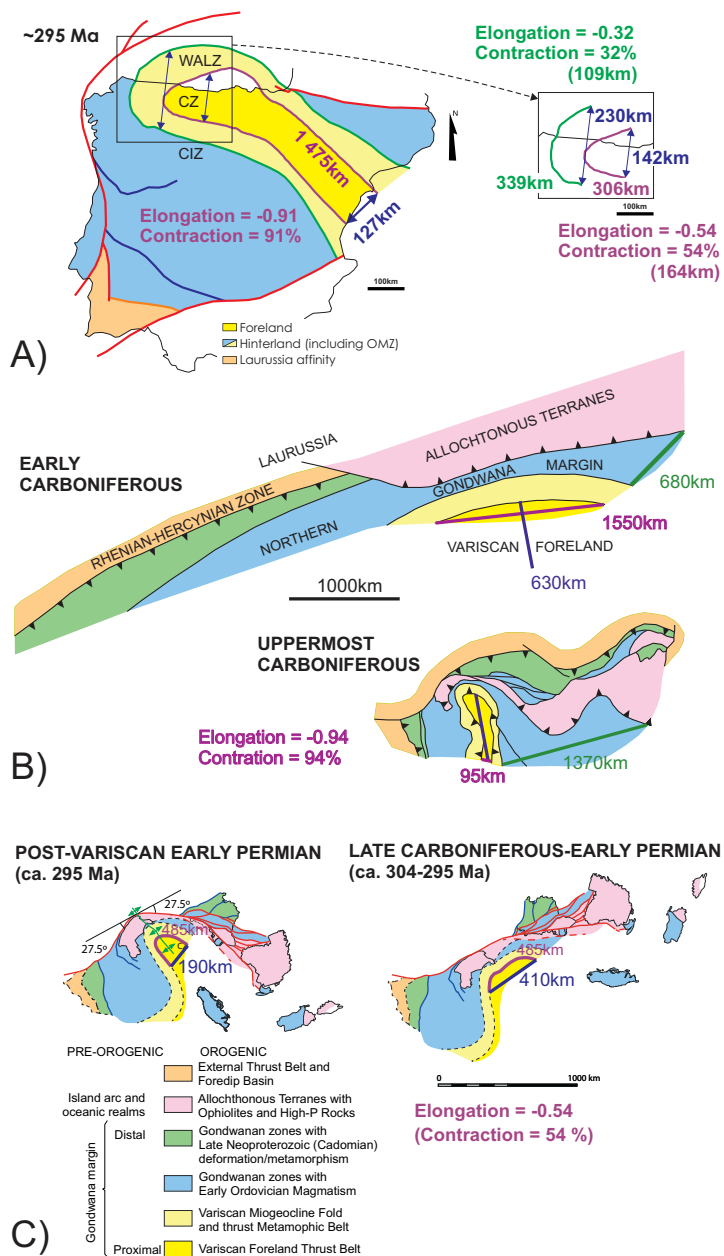


863

864

865 **Fig. 3.**

866

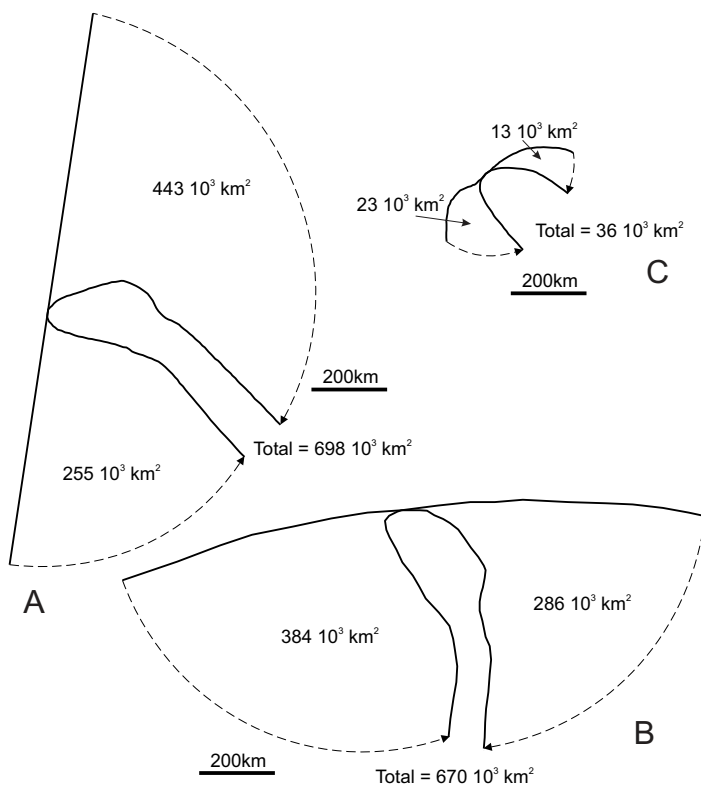


867

868

869 Fig. 4.

870

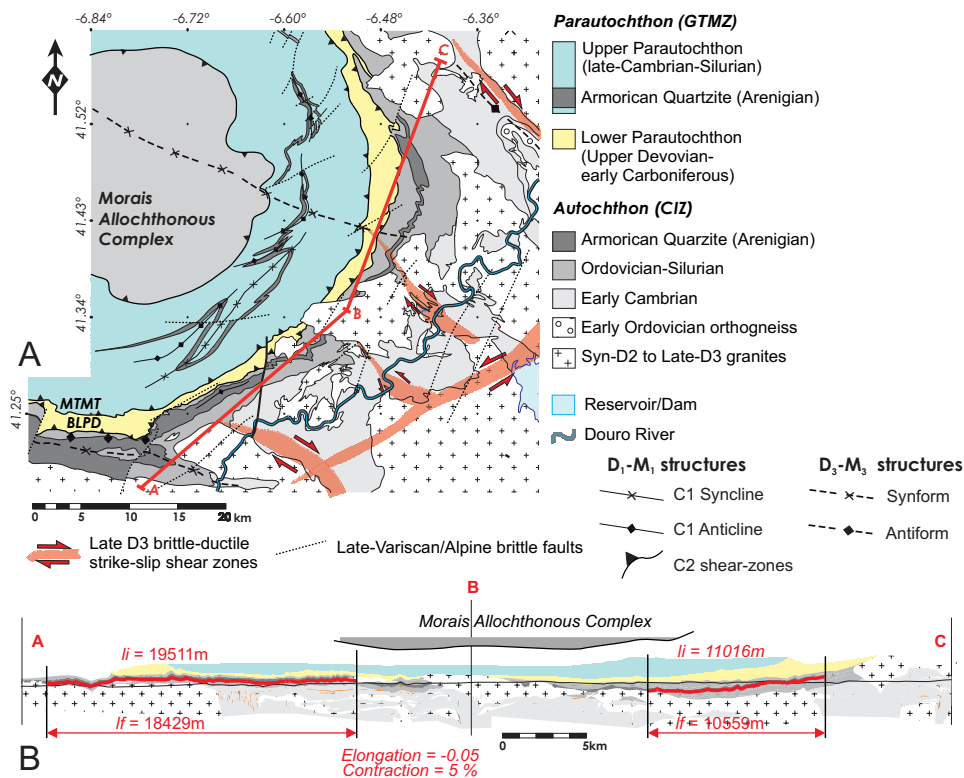


871

872

873 Fig. 5.

874

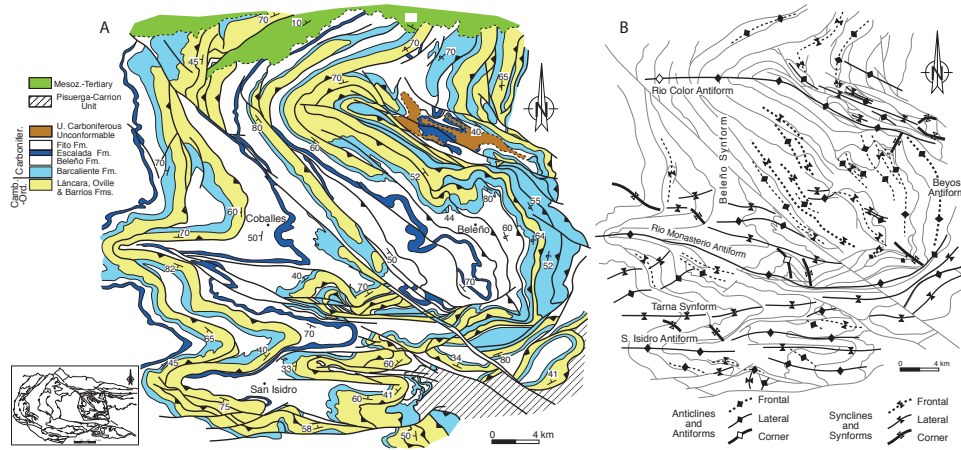


875

876

877 Fig. 6.

878

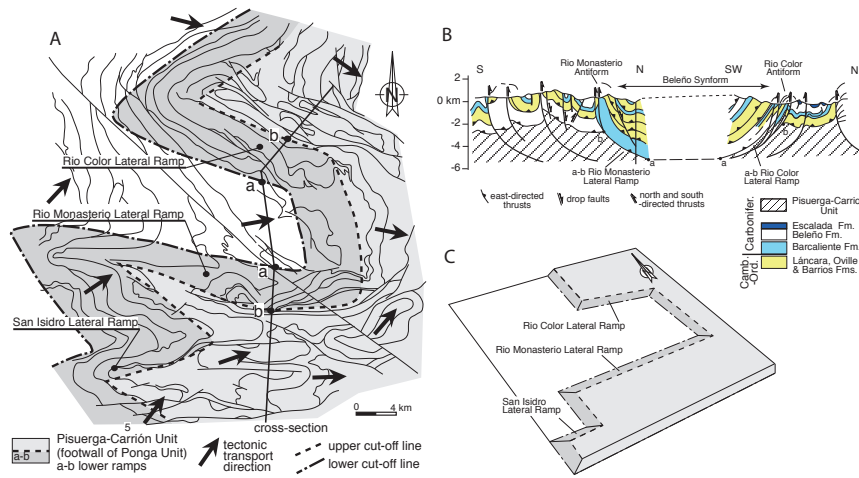


879

880

881 **Fig. 7.**

882

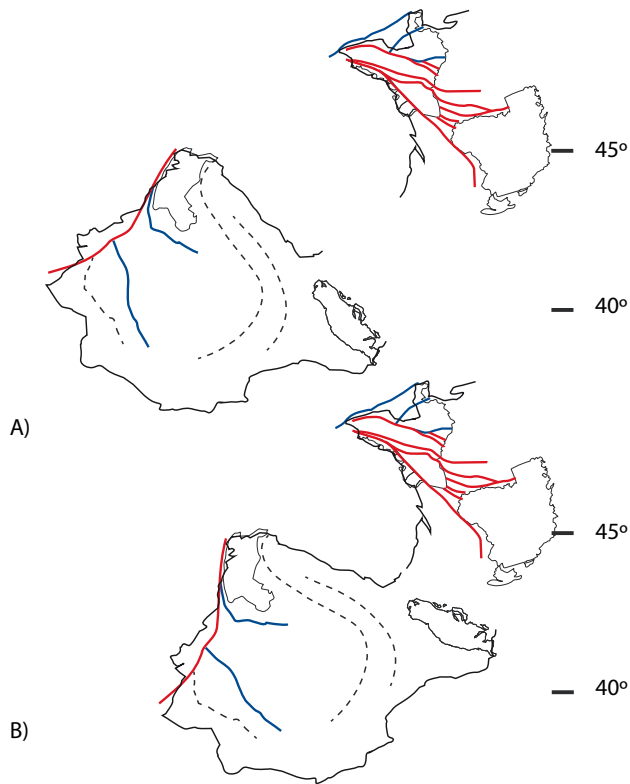


883

884

885 **Fig. 8.**

886



887

888

889 **Fig. 9.**

890

891